Neural Network Theory and Applications 2006

Willard L. Miranker

Yale/DCS/TR-1376
December 2006

Table of Contents

Emergence of Language-Specific Phoneme Classifiers in Self-Organized Maps

Marek W. Doniec
Department of Computer Science
Yale University
New Haven, Connecticut 06511, U.S.A.
marek.doniec@yale.edu

Abstract— **The difference between self-organizing maps based phoneme classifiers that emerge for different input languages is studied. For each such language a self-organizing map is trained on Mel-Frequency Cepstral Coefficient (MFCC) converted auditory input to form a phoneme classifier. Unsupervised learning is used as the training method. The emerging classes are then compared to the classes found in the International Phonetic Alphabet. Particular class differences across languages and speakers are discussed.**

I. Introduction and Related Work

Kepuska et al. [4] have shown that a hexagonal lattice self-organizing map (SOM) shows similar response patterns for the same words and different response patterns for different words. They used 9 repetitions of 20 different words to train and test their SOM. Kumpf et al. [7] showed that using a Hidden Markov Model (HMM) they were able to classify accents within a group of Australian English speakers with an accuracy of up to 85.3%. Kangas [3] has shown that using a time-dependant representation of Mel-Frequency Cepstral Coefficients (MFCCs) can improve phoneme classification from a 10.4% rate error to a 5.0% rate error. However none of these works have compared the resulting classes to the classes found in the international phonetic alphabet (IPA). This alphabet is a much studied and widely accepted classification of phonemes that provides a representation for phonemes of any spoken language [5]. A comparison of the classes learned by a phoneme-recognition SOM to the IPA might reveal strengths or weaknesses of training phoneme classifiers using SOMs and possibly lead to improvement. Further a positive correspondence would suggest that SOMs are capable of capturing the functionality of the human auditory system.

We investigate the differences between phone classes of different languages. The languages are chosen to be different enough so that a native speaker of one language usually has a strong accent in the other language chosen. We first convert the audio signal using Mel Frequency Cepstral Coefficients (MFCCs) which approximate the human auditory system's response and are widely used in speech recognition systems [6], [8]. A self-organizing map is then trained on feature vectors for each of the languages tested. We use unsupervised learning. The classes found in the resulting feature maps are then compared to the IPA by submitting example words for specific phonemes to the trained SOMs or by looking at neurons that respond only to utterances from a particular language. In particular we look for classes that are present in at least one of the trained SOMs but not present the other trained SOMs. In addition we trained an SOM on two languages and examined at neurons that responded only to utterances from one of the two languages. We then identified the phoneme class that these neurons correspond to. Finally we investigate the use of Principal Component Analysis (PCA) to find phoneme classes and to compare phoneme classes from different languages.

The paper is organized as follows. Section II explains how data was collected, preprocessed, and how the SOMs were trained. Section III talks about differences between SOMs that were trained on utterances from different speakers and in different languages. Section IV focuses on differences between languages. Section V examines the use of PCA to detect language and speaker dependencies. Section VI summarizes the results and Section VII contains brief critique.

II. Methodology

First we describe the setup for recording our wave samples. Then we describe how the self-organizing maps were trained, and we introduce a distance measure for the trained SOMs.

A. Recording

Wave files for the experiment were recorded at 8 bits mono with a 22 kHz sampling rate. A simple laptop microphone was used and subjects were given a piece of text from a newspaper article or encyclopedia to read. We recorded two speakers. The first speaker is a native English speaker and was recorded reading English texts. The second speaker is a native German speaker (the author of this paper) and was recorded reading German as well as English texts. For each language / speaker, three wave files were recorded for a total of 9 wave files. Each wave file has a 23 to 33 seconds duration and is about a paragraph of text long. In the following text the abbreviation S_{1E} refers to the first speaker in English. The abbreviations S_{2E} and S_{2G} stand for the second speaker in English and German respectively. $S_{2E,1}$ stands for the first wave file recorded for the second speaker in English, etc. The index for wave files extends to the other abbreviations appropriately.

For the second part of the paper in which we focus on differences across languages another set of data was collected. One native German speaker was recorded a total of 14 minutes reading 16 short text excerpts, 8 in English and 8 in German. The texts were divided into 4 groups, 2 English and 2 German, of which each is 3.5 minutes long. The groups are named $S_E^1, S_E^2, S_G^1, S_G^2$. S_E^1 and S_G^1 were used as the training sets, S_E^2 and S_G^2 were used as the test sets.

B. Training the Self-Organizing Maps

Recorded wave files were first processed using a simple Matlab MFCC library obtained from the internet [9]. The library offers tools to convert the entire wave file into 20-dimensional MFCCs. The signal was converted using a Hamming window of size 32 msec and a hop time of 16 msec. For example, a 32 second wave file would result in 2000 MFCCs of size 20. This data was then presented a total of 20 times to a 10×10 SOM.

C. A Distance Measure

To be able to compare the different SOMs we need a distance measure. For each SOM N and $i \in \{1, ..., 100\}$ let $N(i) \in \mathbb{R}^{20}$ be the weight vector of the i^{th} neuron of N. For $j \in \{1, ..., 20\}$ let $N(i,j)$ be the j^{th} entry of the i^{th} weight vector of N. An advantage of this notation is, that a SOM N can be represented by a 100×20 matrix in which each row represents one neuron. Define the distance between two neurons to be the square of the euclidian distance of their weight vectors:

$$d'(N_1(a), N_2(b)) = \sum_{k=1}^{20} (N_1(a,k) - N_2(b,k))^2$$

Further define the bijective function $m : 1, ..., 20 \to 1, ..., 20$ to be the optimal match between the neurons of two SOMs using the metric just define. This means that m minimizes the following function:

$$d(N_1, N_2) = \sum_{i=1}^{100} d'(N_1(i), N_2(m(i)))$$

Define this optimal match distance to be the distance between two SOMs. We see that this distance measure satisfies the three distance axioms:

1) $d(N_1, N_2) \geq 0$ and $d(N_1, N_2) = 0$ iff $N_1 = N_2$. (Obvious.)
2) $d(N_1, N_2) = d(N_2, N_1)$. (Obvious.)
3) $d(N_1, N_3) \leq d(N_1, N_2) + d(N_2, N_3)$. If m_{12} is the optimal match for N_1, N_2 and m_{23} is the optimal match for N_2, N_3 then the optimal match for N_1, N_3 is at least as good as $m_{23}(m_{12})$.

	Speaker 1 English	Speaker 2 English	Speaker 2 German
Speaker 1, English	11.1053	20.3451	22.0439
Speaker 2, English	20.3451	12.2026	16.4283
Speaker 2, German	22.0439	16.4283	11.5012

TABLE I
DISTANCES FOR SOMS THAT WERE TRAINED ON DATA FROM TWO SPEAKERS. ONE SPEAKER PROVIDED ONLY ENGLISH DATA, THE OTHER PROVIDED BOTH, ENGLISH AND GERMAN DATA. DISTANCES FOR A DATA-SET WITH ITSELF (FOR EXAMPLE THE DISTANCE D(SPEAKER 1 ENGLISH, SPEAKER 1 ENGLISH)) WERE COMPUTED BY COMPARING PAIRS OF SOMS WITHIN THAT DATA-SET. THE AVERAGE OF THOSE DISTANCES IS GIVEN. DISTANCES ACROSS DATA-SET (FOR EXAMPLE THE DISTANCE D(SPEAKER 1 ENGLISH, SPEAKER 2 ENGLISH)) WERE COMPUTED BY MEASURING DISTANCES FOR ALL POSSIBLE MATCHINGS BETWEEN THE SOMS IN THOSE DATA-SETS. THE AVERAGE VALUE IS SHOWN IN THE TABLE.

III. Speaker and Language Dependencies

In this section we examine the differences (distances) between SOMs that are trained on utterances from different speakers and in different languages. We computed the distances between SOMs trained for all nine wave files ($S_{1E,i}$, $S_{2E,i}$, $S_{2G,i}$, $i \in 1, 2, 3$). The process was repeated 5 times to obtain a good average. However it turned out that the SOMs converge so strongly that the differences across two SOMs trained for the same data-set are negligible and thus with a Matlab precision of 4 digits the distances computed for all 5 runs were the same. The results can be seen in Table I.

Note that the absolute value of each distance does not provide useful information, because it depends on the number of neurons used and the representation of the MFCCs. However since the number of neurons and the MFCC representation chosen are the same for all SOMs, comparing two distances is a relevant approach to seek meaning. First we notice that the distance for SOMs trained on the same speaker and the same language are closer to each other then all the other SOMs by at least 34.6%. This means that the metric used does capture some difference between different speakers and languages. Note next that the distance between speakers seems to be larger than the distance between languages by up to 34.1%. This means that our SOMs characterize speaker dependencies more readily than language dependencies. However the SOMs are still capable of capturing the difference between languages for one speaker. Thus we decided to use only one speaker who spoke multiple languages in the balance of the experiments.

IV. Language Specific SOM Areas

In this section we attempted to measure and visualize differences between SOMs that were trained on utterances in multiple languages collected from one speaker. Instead of using our previously defined distance measure, we now use activation maps (specified in this section) to visualize similarities for different language inputs. Because we work with only one SOM, the distance measure does not enter into this part of the study.

A. Training the SOM

Only the wave files S_E^1 and S_G^1 were used to train the SOM for this experiment. Recorded wave files were again first processed using a simple Matlab MFCC library. To reduce the amount of data and keep training times reasonable, a Hamming window of size 100 msec and a hop time of 50 msec was used. This data was then presented a total of 30 times to a 10×10 SOM. Note that the rest of this section is based on the one particular SOM that resulted from such training. However this training process was repeated multiple times and while the resulting SOMs had a different spatial distribution of the neurons, they showed the same properties. These properties are presented in the following subsection.

B. Activation Maps

After training the SOM the four wave files S_E^1, S_E^2, S_G^1, and S_G^2 were processed into MFCCs. The newly trained SOM was used to classify the input vectors. For each input vector the Euclidean distance to all neurons was computed. Each input vector was then assigned the number of the neuron with the smallest Euclidean distance to this input vector (That means this neuron fired for that particular input vector). A count was kept how often each neuron would respond to the input data stream. A separate counter was kept for each of the four data streams resulting from the four wave files. The activation counts were then visualized in two activation maps that are shown in Figure 1. In these maps a neuron's color intensity corresponds to the firing frequency for a given data stream. The intensity of the color red is determined by the firing frequency of that neuron during German utterance, the intensity of green corresponds to English. The color of a neuron moves along the colorspectrum (from red to green) proportionately to the relative frequency of German to English. This means that a brightly red colored neuron responded almost only to German utterances whereas a green colored neuron responded only to data streams of English utterances. Orange and Yellow colored neurons corresponded to a mixture of utterances in both languages. The first activation map (Figure 1(a)) represents the SOMs response to data created from the training set wave files S_E^1 and S_G^1. The second activation map (Figure 1(b)) represents the SOM's response to data created from the test set wave files S_E^2 and S_G^2.

C. Observations

Note that the SOM develops the following four types of neurons:

1) There are a few neurons that do not respond to utterances from either language. For example, neuron $(10, 3)$ is almost entirely dark in both activation maps (For neuron numbering, see the caption of Figure 1). These neurons are most likely a result of the neighborhood-rule, i.e. two neighboring neurons that are far apart 'pull' this neuron into a space that is not used by the input.
2) Most neurons respond in similar ways to utterances in both languages. This is to be expected. Examples are neurons $(1, 1)$ and $(1, 10)$.
3) Some neurons respond almost exclusively to utterances in German. These neurons represent sounds and phonemes that occur predominantly in German. One such neuron is neuron $(1, 9)$.
4) Some neurons respond almost exclusively to utterances in English. These neurons represent sounds and phonemes that occur predominantly in English. One such neuron is neuron $(5, 7)$.

The occurrence of neurons that respond only to utterances in one langauge is a sign that the SOM does develop language-specific regions. To show that these regions are not entirely training-set dependant we produced a second activation map using utterances from a separate test set. As can be expected the activation maps are not identical, however the predominance of certain similarities supports the hypothesis that SOMs develop language specific neurons. In the example illustrated in Figure 1 we can see that for both activation maps the lower right corner is German-dominated and that the center of the SOM is English-dominated. The left top corner responds frequently for both languages. As we shall see later it corresponds to silence (i.e., a pause) between words.

D. A Closer Look at Single Neurons

To illustrate the occurrence of each of the four neuronal classes discussed above and to show that language dependant neurons emerged during training, we have singled out the parts of the wave files that activate certain neurons that are predominant in one or in both languages, as the case may be. We give the total response time of neurons to utterances in different languages. The total response time for a neuron is calculated by multiplying the number of input vectors to which this neuron responded by the stepping size that was used to calculate the input vectors (50 msec).

First we examined the brightly yellow colored neuron number $(1, 1)$. We found that this neuron responded to MFCCs that represented silence. For the training set this neuron responded for a total of 7.6 sec for German and 5.75 sec for English. For the test set the total response time was 12.3 sec for German and 7.75 sec for English. This suggests that when speaking German, our speaker paused longer between words. However pauses might also have been classified by neighboring neurons. Since pauses occur frequently between words in both languages, this neuron $(1, 1)$ is colored a bright yellow in the activation maps.

For further analysis we examined a neuron that exhibited a strong response only for MFCCs created from English utterances. Neuron $(5, 7)$ is colored green and responded a total of 0.05 sec for German and 3.15 sec for English in the training set and 0.05 sec for German and 3.15 sec for English in the test set. Here is a list of some of the words during which neuron $(5, 7)$ fired. Each word is accompanied by a pronunciation transcription as presented by the Merriam-Webster Online Dictionary [10].

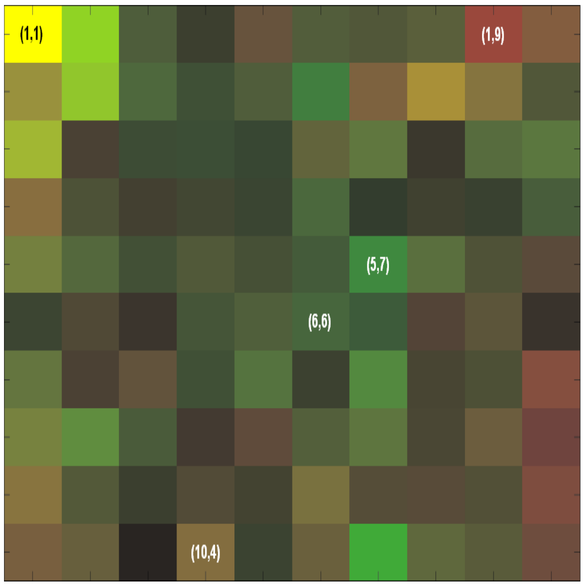

(a) SOM activation map for German and English utterances from the training set.

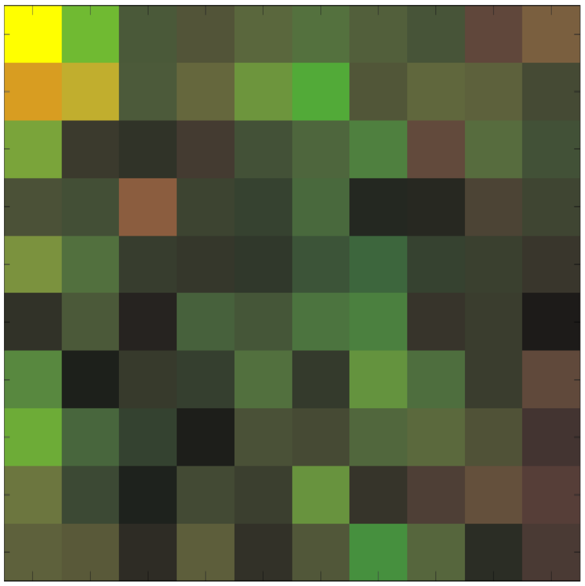

(b) SOM activation map for German and English utterances from the test set.

Fig. 1. These SOM activation maps display the response frequency of neurons to utterances in English (green) and German (red). Yellow denotes a neuron that responded frequently during utterances from both languages. The activation map on the left shows neuron firing frequencies during utterances from the same sample set that was used to train the SOM. The right activation map shows neuron firing frequencies during utterances from a separate test set. The similarities of the images show that certain neurons respond more frequently during utterances in English than utterances in German and other neurons respond more frequently during utterances in German. The neurons are numbered lexicographically in row/column order. The bright yellow neuron at the top in each activation map is thus numbered $(1, 1)$.

- thirty [`'th&r-tE`]
- traverse [`tr&-'v&rs`]
- effort [`'e-f&rt`]
- computer [`k&m-'py`\u-t&r”]
- service [`'s&r-v&s`]
- aircraft [`'er-`\kraft”]

The neuron responded in particular to the [&r], which is pronounced like the ur/er in further.

Neuron $(1, 9)$ was also examined. It is colored a dark red and responded for a total of 4.7 sec for German and 0.45 sec for English for the training set and 4.65 sec for German and 1.0 sec for English for the test set. This neuron corresponded to the nasal [n] sound as in ’nice’ which occurs less frequently in English then it does in German.

Similarly to neuron $(1, 9)$, neuron $(10, 4)$ responded more frequently to German than to English. It represented the [sh] sound as in ’shoe’. It responded for a total of 4.0 sec for German and 2.05 sec for English for the training set and 4.5 sec for German and 2.9 sec for English for the test set.

We also examined the [th] phoneme that does not occur in the German language but frequently occurs in English in words like ’this’ and ’that’. A small test file that contained only that words ’this’ and ’that’ was recorded and the resulting MFCCs were classified with our bilingual SOM. The result is shown in figure 2. This image helped us identify the neuron that corresponded to [th]. This was neuron $(6, 6)$ for this particular SOM. Neuron $(6, 6)$ responded for a total of 0.8 sec for German and 2.35 seconds for English for the training set and 1.45 sec for German and 3.6 sec for English for the test set. While it responded far more frequently to English then to German it is still surprising that this neuron responded to German at all, since the [th] sound does not occur in the German language. We see two possible reasons for this:

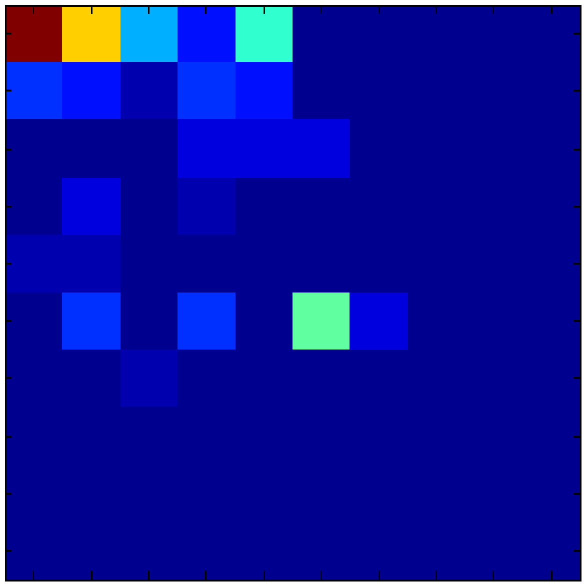

Fig. 2. Activation map for our bilingual SOM in reaction to a recording of ’this’ and ’that’ utterances. Dark blue means no activation, light blue corresponds to medium activation, yellow and red correspond to high activation.

1) The most likely reason is that the speaker recorded was a native German speaker whose pronunciation very likely

	Speaker 1 English	Speaker 2 English	Speaker 2 German
Speaker 1, English	0.2852	0.7209	0.8076
Speaker 2, English	0.7209	0.2146	0.3766
Speaker 2, German	0.8076	0.3766	0.2536

TABLE II
AVERAGE DISTANCES BETWEEN THE FIRST PRINCIPAL COMPONENTS FOR OUR WAVE FILES SORTED BY GROUP (LANGUAGE, SPEAKER). THE ABSOLUTE VALUES ARE OF NO MEANING, HOWEVER THERE IS A SIGNIFICANT DIFFERENCE BETWEEN THE DISTANCE FOR SPEAKERS AND THE DISTANCE FOR LANGUAGES. THIS SUGGESTS THAT PCA IS ABLE TO CAPTURE SPEAKER DIFFERENCES.

biased the result.

2) The resolution of the SOM might cause two sounds to be classified by one neuron. Thus the same neuron might respond to similar sounds like [v].

V. PRINCIPAL COMPONENT ANALYSIS

We also investigated the use of Principal Component Analysis (PCA) to recognize speaker or language dependencies. PCA is a good candidate because it both extracts the most significant components and allows for a dimensionality reduction of the data. We hoped that we could identify components that would help identify the speaker or the language.

The input wave files were again transformed into MFCCs using 100 msec Hamming windows and a hop time of 50 msec. We use the files ($S_{1E,i}$, $S_{2E,i}$, $S_{2G,i}$, $i \in 1, 2, 3$). We then applied PCA to each data stream and saved the principal components (20 components for each file, each component of size 20). For each principal component and each pair of files we computed the Euclidian distance giving a total of $9 \times 9 = 81$ distances. The distances were then averaged over comparisons between files from the same group (there are three groups: S_{1E}, S_{2E}, and S_{2G}). This resulted in 20 tables, one for each principal component. Each table gives the average distances for this particular principal component between languages and speakers. We found that the first component represented the distances between speakers well as can be seen in Table II. However none of the components seemed to represent differences in language.

In a second analysis we used PCA to reduce the input space for our SOM training algorithm. For this the MFCC transformed files S_E^1, S_E^2, S_G^1, and S_G^2 were concatenated and PCA was applied to the resulting data stream. This time the representation in principal components was input to the SOM as input. The results were similar as in the that in Section IV.

However we found the following problem in utilizing PCA together with SOMs. PCA generates different principal components for different input files as shown in Table II. This results in the problem that if we transform two files separately then their representation in their respective principal components are of no value to the SOM, because they are independent of each other. We tried to represent additional data in the principal component space of the training data but only with marginal results.

VI. SUMMARY OF RESULTS

We showed that training SOMs on MFCCs results in SOMs that are both, speaker and language dependant. This result was obtained by comparing the SOMs with a specified metric. This suggests that SOMs can be used to differentiate between languages and between speakers.

We further showed that SOMs do capture differences between languages that can be easily made discernable. In particular we showed that if an SOM is trained with two languages then some neurons represent sounds that are unique or predominant in one of the languages. An additional result was that independently of the language used, the SOM has certain neurons that correspond to silence (a pause) and are activated more frequently than other neurons in the same SOM.

We showed that PCA might be able to extract speaker differences but most likely is not suitable to extract language differences. Further we explained that it is not possible to use PCA to preprocess the input to the SOM training algorithm because PCA will generate different principal components for two separate input samples. Thus representing each sample in the principal component space does not allow for a good comparison of two different samples.

VII. DISCUSSION

The results suggest that training an SOM on unlabeled speech data can result in the formation of a phoneme classifier in which groups of neurons or single neurons correspond to different phonemes. Although these phonemes are not labeled they seem to represent the phoneme space of spoken languages well. These SOMs help to further reduce the dimensionality of the input and could be of use for further classification and speech recognition tasks. The advantage over existing work is that our system uses unsupervised learning and thus needs no feedback.

We have found that the SOMs capture speaker as well as language differences. This suggests that an SOM might be used to discern certain simple classes of speakers. An analog of this is the preferential response of infants to their mother's voice as found by Mehler et al. [12].

The language differences captured suggest that an SOM adapts to a certain language and its phonemes. This is also similar to findings in infants who habituate themselves to a particular set of phonemes and tend to attenuate non-native phonemes during advanced langauge learning [11]. Further we have shown that if trained with two languages at once an SOM can learn both phoneme sets and even distinguish between sounds that occur only in one of the languages. For future work we envision a system that learns to differentiate between several different languages based on the firing pattern of a trained SOM.

Another utilization of such an SOM could be speech segmentation. We observed that the neurons representing silence in the SOM fire more frequently then any other neuron (see Figure 1). This suggests that if indeed silence is the predominant feature vector, our system has developed a set of neurons that represent word-boundary signals. So not only does our SOM learn to classify phonemes but it could provide a subsequent speech recognition system with word boundary information.

We showed that PCA is not well suited for preprocessing the input for the SOM in the case of building phoneme classifiers. We believe however that PCA might serve to extract principal components from a large data set for in the identification of speakers. The reason that PCA demonstrated no utility for preprocessing is that different input files produced different principal components. This happens especially if the input files are small and thus provide only a small sample of training data. Further study will show whether the principal components will tend to stabilize for large bodies of data (multiple hours of recordings for each speaker / language combination). If such fixed points exist they might prove useful for preprocessing the speech signal.

Future work should include a more detailed analysis of the exhibited behaviors. The results obtained in this study are based on noisy data that was collected under suboptimal conditions from only two subjects. We believe that a large scale study employing data from many subjects might reveal additional features and allow testing of the interaction between different languages and speakers. The reason that we used only one speaker for the second part of the study is that currently there is no good method for extracting speaker independent feature vectors from speech. MFCC still captures the base frequency and possibly other speaker dependent features and thus does not allow for efficient comparison of languages across speakers. Current work on speaker independent phoneme classification usually trains classifiers on a large body of subjects [13]. While these classifiers learn to generalize across different subjects, they are still presented with speaker-dependent input such as MFCCs. A similar approach might be used in combination with the methods presented here. Naturally this would require a large body of data.

We have shown that the unsupervised learning of SOMs with as few as 100 neurons enables extraction of speaker and langauge differences. We showed that some can extract additional useful information such as word boundaries. Thus SOMs are well suited for use in unsupervised learning systems for word grounding (learning the meaning of words) and language recognition. We have also shown that SOM phoneme recognizers show learning and recognition behavior similar to that of human infants.

References

[1] C. Yu, D. H. Ballard and R. N. Aslin, *The Role of Embodied Intention in Early Lexical Acquisition*, Coginitive Science, 29(6), 961-1005, 2005.

[2] D. K. Roy and A. P. Pentland *Learning words from sights and sounds: a computational model*, Cognitive Science, 26(1), 113-146, 2001.

[3] J. Kangas, *Phoneme recognition using time-dependent versions of self-organizing maps*, In Proceedings of the International Conference on Acoustics, Speech and Signal Processing, p. 101-104, Toronto, Canada, May 1991.

[4] V. Z. Kepuska and J. N. Gowdy, *Investigation of phonemic context in speech using self-organizing feature maps*, IEEE International Conference on Acoustics, Speech and Signal Processing, ICASSP ’89, Glasgow, Scotland, May 1989.

[5] International Phonetic Association, *Handbook of the International Phonetic Association - A Guide to the Use of the International Phonetic Alphabet*, July 1999.

[6] Z. Fang, Z. Guoliang and S. Zhanjiang, *Comparison of different implementations of MFCC*, Journal of Computer Science and Technology, 16(6), 582-589, 2001.

[7] K. Kumpf and R. W. King, *Automatic accent classification of foreign accented australian english speech*, In Proceedings of 4th International Conference on Spoken Language Processing, Philadelphia, USA, October 1996.

[8] *Mel frequency cepstral coefficient*, Wikipedia, http://en.wikipedia.org/wiki/Mel_frequency_cepstral_coefficient, 2006.

[9] *PLP and RASTA (and MFCC, and inversion) in Matlab*, D. Ellis, http://labrosa.ee.columbia.edu/matlab/rastamat/, 2006.

[10] *Merriam-Webster’s Online Dictionary*, www.m-w.com, 2006.

[11] D. Burnham, *Language specificity in the development of auditory-visual speech perception*, R. Campbell & B. Dodd (Eds.), Hearing bye eye II: Adances in psychology of speechreading and auditory-visual speech. Hove, england: erlbaum UK, pp. 27-60, 1998.

[12] J. Mehler, J. Bertonicini, M. Barriere, *Infant recognition of mother’s voice*, Journal of Perception, 7(5):491-7, 1978.

[13] M. Antal, *Speaker Independent Phoneme Classification in Continuous Speech*, Studia Univ. Babes-Bolyai Informatica, Vol. XLIX, No. 2, pp. 55-64, 2004.

Modeling Child Development using a Game Theoretic Approach and Genetic Algorithm

Laura J. Gehring

Abstract— **A child's development of mind is studied using iterations of a Prisoner's Dilemma game in conjunction with a genetic algorithm. Situations where a poor parent is replaced mid-set with a near optimal parent are investigated. This provides a model for the situation where a child in the care of an individual suffering from a form of psychopathy such as depression are witness to their recovery or removed to more attentive care. A genetic algorithm is used to represent the child's memory throughout parental development. As hypothesized the model demonstrates rates of change in fitness and mental development which correlate to the length and quality of care received by the child in each distinct section of the trial.**

Index Terms—**Parental Psychopathology, Theory of Mind, Game Theory**

I. Introduction

As adults, the vast majority of humans realize that there is not one collective mind in use by the entire population. Beliefs and the substance of knowledge vary from person to person. Such an awareness of the individuality of others does not seem to be inherent from birth, but develops as a child does with common tests for this ability usually being successfully completed by children who are, at the very youngest, 3 to 4 years old[2]. Understanding how such ability arises remains a topic of continued psychological research. Studies have shown that one factor affecting the time before emergence of a full theory of mind is the amount and type of discourse a child is exposed to[4]. Interactions between parents and children can be grouped into two broad categories, "mentalizing" and "non-mentalizing"[5]. Mentalizing responses to a child would include any in which a caregiver recognizes and draws attention to the child's state of mind, and how it relates to their actions and reactions to events. Non-mentalizing responses deal more directly with actions, events, and consequences with no reference to how a child's mental state was involved. The ratio of mentalizing to non-mentalizing interactions children and caregivers engage in would necessarily vary due to environmental factors. However, not all children are given the opportunity to interact with a "normal" adult.

We will develop a model for the interaction of a normal child with a normal parent and contrast this with relations formed by a child with some imperfect parent. Such a model could be equated with situations in which a child is interacting with a caregiver suffering some form of psychopathology, such as depression, which affects ability to interact in a manner comparable to that accomplished by normal adults. Interactions with such "semi-developed" adults should delay child's development[1]. Further, we will model the effects of switching from a semi-developed parent to a fully-developed one such as would occur in a real-life situation when a parent seeks help for their condition or when children are moved to a more stable environment. Such a situation should influence the child's rate of development. An initial drop in development could be expected directly after such a shift followed by an increased rate of development correlating with the increased efficacy of the current caregiver over the previous.

A game theoretic methodology such as the one outlined by Mayes and Miranker[5] will be used to model this interaction and the resulting development of the child. Here a version of the Prisoner's Dilemma was suggested to model the interaction between caregiver and child while the development of mind would be represented by the convergence of a child's strategy of play to one beneficial in the current context. The child's memory of past exchanges is represented with a genetic algorithm and is used to help choose the child's course of action

II. The Model

A. Initializing Prisoner's Dilemma

In the interest of clarity, female pronouns will be used to refer to the parent while male pronouns will be used in reference to the child from this point on. In the model, the parent and child each have two options. She has the option of ignoring the child which requires an absolute minimal effort, or paying attention to him which does require effort. The child's two options are to use his intuition which is associated with a minimal cost, or to use his mind, which would use more energy. Both parties have the goal of expending as little effort while reaping the benefits of the other's efforts. The ideal situation, from a parent's perspective, therefore, would be one in which the child is constantly ignored and yet continues to use his mind. Using the mind causes him to mature. The child's decision to use mind would therefore benefit the parent

Manuscript received November 28, 2006.
L. J. Gehring , junior at Yale Universtiy(e-mail: laura.gehring@yale.edu).

by reducing the period of time in which he was dependent on her parents. The child's ideal situation, in contrast, would be to continuously choose to use intuition and receive attention from the parent. In such a case, the child is not neglected and does not have to pay for the attentions received with the cost of using his mind instead of intuition. Remaining possible scenarios are that both parties choose actions requiring effort or that both parties choose actions requiring minimal effort. These two courses result in changes which are equal in both the parent and child. These relative costs can be assimilated into the payoff matrix of Table I.

Table I: Child\Parent Action Payoffs

Child\ Adult	Attend	Ignore
Mind	R, R	S, T
Intuition	T, S	P, P

When values of T>R>P>S are implemented a true Prisoner's dilemma is created which models the previously defined interactions as desired. The value each participant in the game receives hinges on the actions of their opponent. In this case, the best results for an individual are the product of successfully tricking the other player into doing more work while engaging in less itself. The opponent then receives the lowest possible return value. In the real world, such actions result in a loss of trust. A rational agent would learn from such an experience and when confronted with that same type of situation would be more apt to anticipate another deception. The logical course would be to minimize losses by engaging in the less expensive activity. This kind of activity would naturally degrade into the (P,P) situation. Cooperating to achieve the (R,R) situation would benefit both parties more in the long term, but is much more difficult to achieve because of the increased risk associated with that position.

B. *Memory*

Each iteration of the Prisoner's Dilemma will result in a move by the child and a reaction from the parent. To isolate the reactions of the child, it will be assumed for this model that the parent's strategy will not be affected by game play and only alters at the designated time when it is shifted to its more/less optimal counterpart. For ease of implementation and because of its proven efficacy, an optimal parent will use the tit-for-tat strategy and respond to the child's action with an action of corresponding cost. For example, if the child chooses Mind she will counter with Attend while if he opts for Intuition she will choose Ignore.

When a child begins, it has no memory and is obliged to make a random play. At the end of the iteration, it receives the payoff determined by the above matrix. This amount is added to the child's fitness level, which is initially set to 0. This fitness level provides an indication of how well he understands his adversary. A high fitness value results from typically high values returned after participating in the Prisoner's Dilemma and indicates a better understanding of the strategy being used by the opponent and its successful exploitation. At this point a decision, on the basis of payoff and a random variable, is made to either include the play sequence in memory or to discard it.

A child's memory is represented by a tree. Each node represents a point of play and has two branches which represent the two possible actions that the child may take at that instant. Additionally, a weight, initially set to zero, is associated with each of these options. These two branches lead to two more nodes each with two more branches and so on. The weight associated with each branch signifies how successful a given choice at this node has been at increasing the child's fitness in the past. All weights are initially set to 0, meaning that there is neither benefit nor loss associated with each choice at that point. However, as the child ages and creates memories, these weights come to reflect the outcomes of previous decisions. When an event is committed to memory the outcome is associated not only with the most recent action, but also with the sequence of deeds leading up to the most recent choice. Weights corresponding with the action chosen must be updated in each of the specific nodes reached by following the increasingly complex sequence of previously chosen actions up to the depth of the child's ability to recall specific past choices. For example, if he could only remember the last four choices made, it would be necessary to change the weights of those nodes reached by walking the last 4, 3, 2, and 1 actions chosen by the child.

If a child chooses to use its memory, a number of past sequences equal to the child's memory recall level are summoned from the end of the record of past child choices. Using these, the most beneficial sequence may be selected using a genetic algorithm, and a choice between the two current options is returned. Weights of the associated sequence of plays and the child's fitness are altered based on payoff garnered as a result of the choice.

C. *Introduction of Psychopathy*

Each run of the simulation will consist of time spent with an optimal parent and time with a suboptimal parent. The optimal parent will use a pure tit-for-tat strategy while the suboptimal parent will follow a similar strategy, but interspersed with noise created by random deviations from that strategy. The amount of deviation will be controlled between trials to investigate effects of more and less deviation from the tit-for-tat strategy. The actions of the suboptimal parent will be determined by the value of a randomly generated variable, which when greater than some threshold will choose to play randomly rather than use tit-for-tat. This threshold may be increased (to increase optimality) or decreased (to increase the number of random plays).

The model will consist of having the child play the suboptimal parent for a number of iterations before switching to the optimal parent and measuring how long it takes the child to reach a strategy for use with the fitter parent which provides the highest payoffs as they have been previously defined. Each segment of the experiment will consist of 50 distinct games so that an average course of development less skewed by chance may be obtained. Each game will be composed of 100 iterations of the Prisoner's Dilemma, or 200 combined moves made by the child and parent. Each game will begin with a fresh child with no previous memories and no record of past moves. The goal will be to determine and compare the effects of exposure to suboptimal parents of varying degrees of degradation on the child's development and ability to recover when later exposed to optimal parenting.

III. Experiment

A. Overview

Initially, the model was run solely with the optimal parent and subsequently completed runs with each of the suboptimal parents to be investigated to create points of comparison. Next, the game was executed several times with differing levels of degradation in the initial suboptimal parent before switching to the optimal caregiver after 50 iterations involving the suboptimal player. After that, the length of exposure to the suboptimal parent was modified to evaluate the effects of varying amounts of exposure to the same suboptimal caregiver. Finally, the effects of exposing a child to a more effective, though still suboptimal, parent following 50 iterations with a suboptimal parent will be explored.

During each of these trials, records will be kept regarding the child's fitness which correlates with the values received from engaging in the Prisoner's Dilemma. Also, Maturity of the mind will be recorded. Maturity may be defined as the number of times he has chosen mind over intuition. As the child plays, strategies should form, which when followed, cause the child's fitness to grow more quickly than when playing randomly. Since a tit-for-tat strategy is being used, the response strategy for the child is to always choose mind. Playing intuition against a parent utilizing a strict tit-for-tat strategy will always yield a lower payoff than that achieved by playing mind. The emergence of this strategy will also be monitored during each of these trials and recorded. Point of emergence will be defined as the point at which child chooses to play mind over intuition during ten consecutive iterations. As the optimality of the parent decreases and the number random plays made by the parent increases, the value of constantly choosing mind degrades and children are slower to adopt it because of its decreased utility. In fact, those children paired with a parent who makes only random plays will soon adopt the opposite strategy of always choosing intuition so as to minimize losses against this irrational agent.

B. Optimal Exposure

Under optimal conditions, the parent counters all moves of the child using a pure tit-for-tat strategy. Results for these trials are displayed in Tables II.a-c. Here the strategy arrives very early on averaging at around 4.68 iterations into the trial with a standard deviation of 3.71. The average maturity, or number of times the mind was chosen, at the end of the trial was 97.54 with a standard deviation of 1.25 while fitness at the end of the runs averaged 95.08 with a standard deviation of 2.50.

C. Varied Suboptimal Exposures

To contrast with the optimal parent, trials of 100 iterations were also performed with parents of varying levels of random play. Information from these trials is summarized in Tables II.a-c alongside information from the optimal trial as a point of comparison.

Table II.a: Emergence of strategy

Parent Exposure	Mean Number Plays to Emergence	Stand. Dev.	Non-maturing
Optimal	4.68	3.71	0
70% Optimal	10.2	8.25	0
50% Optimal	22.26	20.88	0
30% Optimal	66.08*	20.25*	21 (42%)
Random Play	---------	----------	49 (98%)

*To make the mean and standard deviation of trials where many runs did not converge more meaningful, a value of 100 was substituted as the point of maturation for such runs. This helps offset the somewhat lesser values for each of these that would otherwise occur.

Table II.b: Maturity

Parent Exposure	Mean End Maturity	Stand. Dev.
Optimal	97.54	1.25
70% Optimal	95.04	3.61
50% Optimal	88.22	10.33
30% Optimal	55.34	29.77
Random Play	7.9	6.34

Table II.c: Fitness

Parent Exposure	Mean End Fitness	Stand. Dev.
Optimal	95.08	2.50
70% Optimal	46.7	12.62
50% Optimal	21.06	14.85
30% Optimal	1.98	14.23
Random Play	36.88	20.24

It is important to note, that when a completely random parent is used with no adherence to a tit-for-tat strategy that the child does in fact reach an effective strategy of sorts, it simply never uses its mind and maturity, as it is measured, suffers. With random plays this would equate to an overall increase in fitness when the values of the payoff are arranged symmetrically and the parent gives attention and ignores equally. However, this strategy is relatively useless against a parent with a strategy like tit-for-tat where the child will never receive a reward, or positive payoff, for not using his mind. As the amount of random activity is increased the fitness of the child initially decreases as it makes the transition between two very different strategies which is why the fitness is so low when the parent is only playing at a 30% optimal level. Further decreases in random play firmly establish an effective strategy to be used in conjunction with tit-for-tat. Graph III in the appendix illustrates these two clear strategies adopted by the child and the ways in which fitness and maturity are affected.

It is also appropriate that the standard deviation for aspects of measurement like fitness and maturity tend to increase as random play is increased. The exceptions to this rule tend to occur at points of key change such as the instance where there are an unusual number of trials which never converged to the strategy and thus affected the mean emergence and standard deviation.

D. Varied Suboptimal Parenting followed by Optimal Parenting

The ability of a child to converge upon the ideal tit-for-tat response strategy following exposure to varied levels of suboptimal parenting was examined by having the child interact for 50 iterations of the game with parents of varying degrees of random play before being exposed to the optimal parent for the remaining 50 iterations. Results from these trials, summarized in Tables III.a-c and Graph I of the appendices, highlight the unique changes in fitness that accompany such changes in strategy. Notation of the type of Parent Exposure is defined in the form Split-X-Y where X/Y refers to the number of iterations performed by the first parent / her optimality. For example "Split-10-70" would denote trials in which a parent adhering to the tit-for-tat strategy 70% of the time was used for the first 10 iterations and a completely optimal parent was used for the remaining 90.

Table III.a: Emergence of Strategy

Parent Exposure	Mean Number Plays to Emergence	Stand. Dev.	Non-maturing
Optimal	4.68	3.71	0
Split-50-70	9.74	7.02	0
Split-50-50	21.3	18.46	0
Split-50-30	43.28	23.25	0
Split-50-rand	70.42	12.03	0

Table III.b: Maturity

Parent Exposure	Mean End Maturity	Stand. Dev.
Optimal	97.54	1.25
Split-50-70	94.96	3.60
Split-50-50	87.86	12.28
Split-50-30	70.24	17.40
Split-50-rand	41.56	12.67

Table III.c: Fitness

Parent Exposure	Mean End Fitness	Stand. Dev.
Optimal	95.08	2.50
Split-50-70	72.16	8.44
Split-50-50	57.3	11.41
Split-50-30	39.46	12.12
Split-50-rand	35.86	8.70

As expected, the rates of emergence of a strategy, maturity, and fitness are inherently linked with the optimality of the parent with means for these three points of measurement increasing as random play is decreased. Also, again the standard deviations consistently decrease as random play does so in most instances. The most interesting point in this data occurs once again in the area at which there seems to be a boundary between two very distinct strategies whose respective execution seems mutually exclusive. Once again, there is a very real drop in the mean fitness at the level of play where a 30% optimal parent is used, also the level with the highest standard deviations across all points of comparison. It is also interesting to note, that while mean fitness seems to be linearly associated with decreasingly random plays, the values measuring maturity seem to decrease slowly before dropping off dramatically as the amount of random play is increased while emergence of strategy follows an inverted version of this pattern.

E. Varied Length of Exposure to Suboptimal then Optimal Parenting

The effects of length of exposure are examined using varied lengths of exposure time with a 70% random parent followed by an optimal caregiver. Such situations are represented in Tables IV.a-c by an identifier such as "Split-10-30" which would denote that the first 10 iterations of each trial were held between a child and parent who uses the tit-for-tat strategy on 30% of the iterations and randomly selects a course of action 70% of the time. The remaining 90 iterations would then utilize the optimal parent who consistently uses tit-for-tat.

Table IV.a: Emergence of Strategy

Parent Exposure	Mean Number Plays to Emergence	Stand. Dev.	Non-maturing
Optimal	4.68	3.71	0
Split-10-30	12.72	4.51	0
Split-20-30	21.02	10.23	0
Split-30-30	28.50	13.14	0
Split-40-30	34.42	17.15	0
Split-50-30	43.28	23.25	0
Split-100-30	66.08	20.25	21 (42%)
*values of 100 are substituted as mean trial convergence point for trials that do not converge			

Table IV.b: Maturity

Parent Exposure	Mean End Maurity	Stand. Dev.
Optimal	97.54	1.25
Split-10-30	92.32	4.04
Split-20-30	87.48	6.88
Split-30-30	82.26	10.55
Split-40-30	77.06	12.51
Split-50-30	70.24	17.40
Split-100-30	55.34	29.77

Table IV.c: Fitness

Parent Exposure	Mean End Fitness	Stand. Dev.
Optimal	95.08	2.50
Split-10-30	85.6	6.27
Split-20-30	75.14	7.89
Split-30-30	64.16	8.45
Split-40-30	52.68	9.15
Split-50-30	39.46	12.12
Split-100-30	1.98	14.23

The emergence strategy is particularly interesting. The data suggests that the child was on the verge of converging and only needed the smallest of nudges created by an optimal parent to achieve this. Particularly, the points of achievement were all recorded as the point at which a sequence of 10 or more iterations achieved a stable state. With this in mind, note that the mean point of emergence for all of the trials involving an optimal later parent are within 10 iterations of the point at which this change was made. As more trials are performed with the 30% optimal parent, more trials will converge before reaching the point at which the optimal parent takes over. Also note that the differences in the mean points of emergence of those trials which were subjected to the optimal parent are roughly linear. This is also true of the corresponding differences in mean values of maturity and fitness.

F. Suboptimal Parenting followed by better Parenting

As one last point of comparison, the effects of interactions with a suboptimal parent with a rate of optimality of 30% for fifty instances of the Prisoner's dilemma was replaced in the last 50 iterations of the game with parents of varying optimality to see how such a change would affect the child. Observations from these trials are summarized in Tables V.a-c and noted in the form Split-X-Y-Z. X refers to the number of iterations performed by the first suboptimal parent, Y is the optimality of that parent which in this case is always 30%, and Z is the optimality of the parent which will be used in the remaining iterations.

Table V.a: Emergence of Strategy

Parent Exposure	Mean Number Plays to Emergence	Stand. Dev.	Non-maturing
Split-50-30-100	43.28	23.25	0
Split-50-30-70	46.82	26.39	0
Split-50-30-50	62.32	29.74	11 (22%)
Split-50-30-30	66.08	20.25	21 (42%)
*values of 100 are substituted as mean trial convergence point for trials that do not converge			

Table V.b: Maturity

Parent Exposure	Mean End Maurity	Stand. Dev.
Split-50-30-100	70.24	17.40
Split-50-30-70	68.2	18.28
Split-50-30-50	60.18	24.01
Split-50-30-30	55.34	29.77

Table V.c: Fitness

Parent Exposure	Mean End Fitness	Stand. Dev.
Split-50-30-100	39.46	12.12
Split-50-30-70	20.14	14.36
Split-50-30-50	-2.38	14.74
Split-50-30-30	1.98	14.23

It is interesting that when an optimal parent is replaced in the second half of the run by one whose optimality is only 70% there is relatively little effect in either the emergence of a strategy or the evolution of the mind as measured by maturity. As can be seen in Graph II of the appendices, the line of ascent is smoother for the trial utilizing the optimal parent for the last

50 iterations, and fitness suffers as the parent's playing ability decays. Results in areas such as end maturity, on the other hand are much the same.

However, as further demonstrated by the comparison, results achieved by a later parent at 50% optimality seem rather abysmal in categories such as fitness while there is also a substantial drop in measures of maturity and a substantial increase in the amount of time needed to converge to the tit-for-tat based strategy.

Trials only utilizing a 50% optimal parent converge after an average of 22.26 iterations while 70% optimal parents converge after 10.2. When these same two are made to follow the 30% optimal parent, the difference between rates of convergence becomes 15.5. The small difference between rates of convergence for the trial with a 50% optimal parent used in the second half and one where a 30% optimal parent continues to be used is also telling. It seems that the ability to reduce the effects of poor previous efficacy is not linear. Of course, the standard deviations for all of these trials are quite large making accurate in-depth analysis difficult.

IV. Conclusion

Results illustrate, as common sense would suggest, that both the quality and level of exposure to suboptimal caregivers is reflected in the child's development. It is comforting, however, to realize that while consistent childcare is best for the development of a distinct, effective strategy on the part of the child, complete consistency is not necessary for its achievement. Rather, it seems that the consistency must simply outweigh the loss the child would expect by not conforming to the strategy being deviated from. This is a necessary evolutionary development given that the overwhelming majority of parents would find it impossible to always behave fairly and in a tit-for-tat fashion throughout childhood. It is also interesting to note, that for the intent of the parent, a pure tit-for-tat strategy does not seem to be most advantageous when cost and resulting maturation are compared.

V. Appendix

Graph I

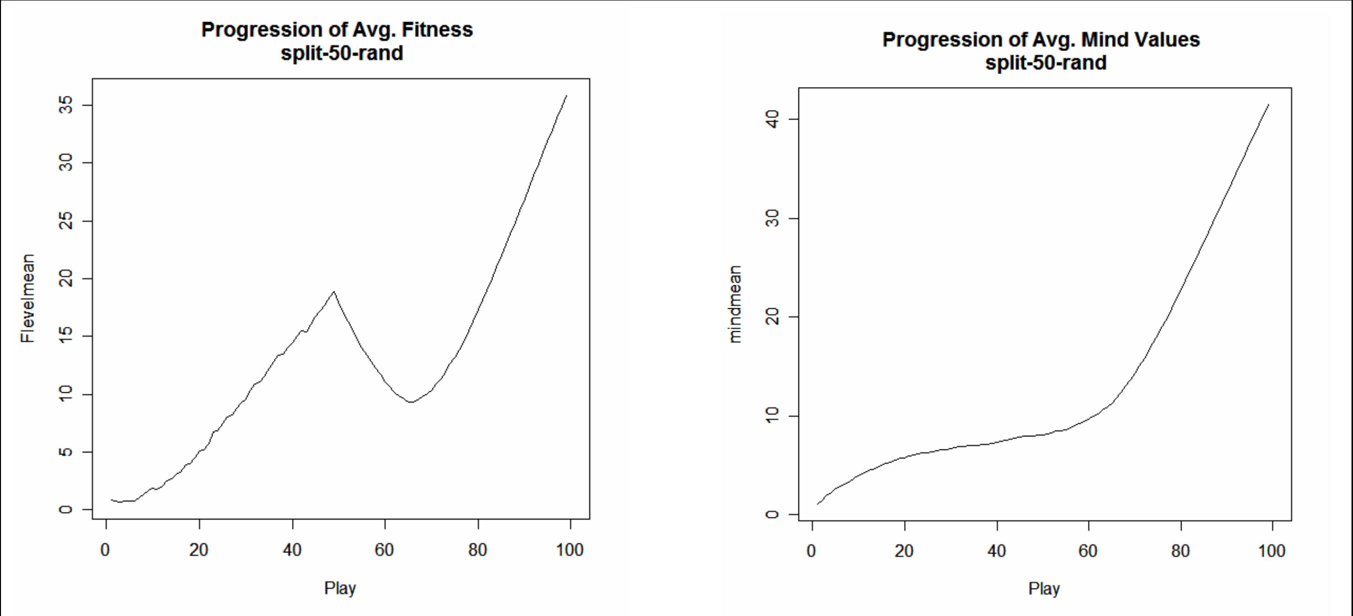

Graphs showing the average progression of fitness and Mind or maturity values in a situation in which a random agent is utilized for the first 50 iterations, after which an optimal (tit-for-tat) parent is substituted. Note the dramatic dip in fitness that occurs on the left at the point where the parents are exchanged. The child's fitness decreases after the initial switch before rising steeply once more. The right demonstrates the sloping off of mind usage when exposed to a random agent followed by increased choosing of Mind in the presence of the optimal parent.

Graph II

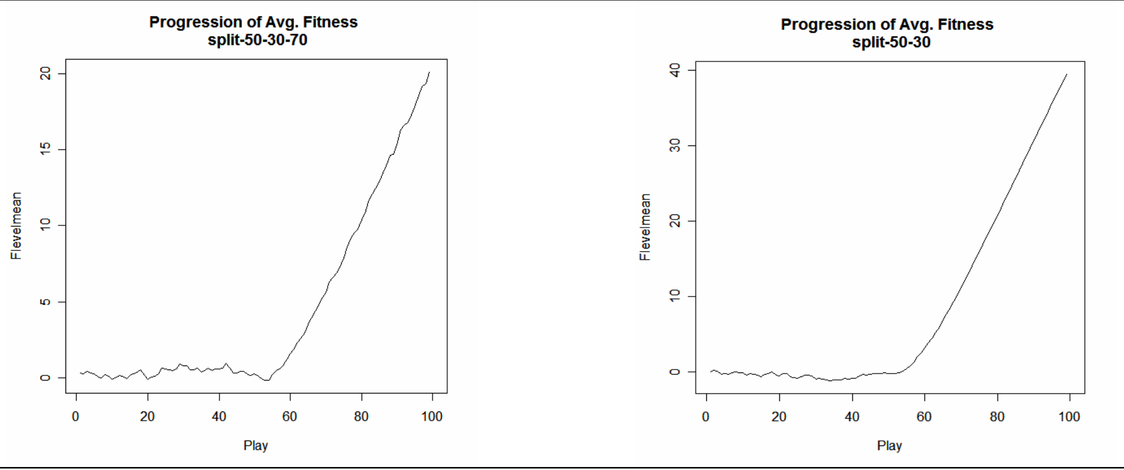

Both graphs illustrate the situation where a 30% optimal parent plays the first 50 iterations. However, on the left, this suboptimal parent is replaced by a parent who is 70% optimal while that on the right was replaced by an optimal parent. The increase in fitness is smoother and more dramatic on the right, but both demonstrate a definite improvement in the child's fitness resulting from their respective changes.

Graph III

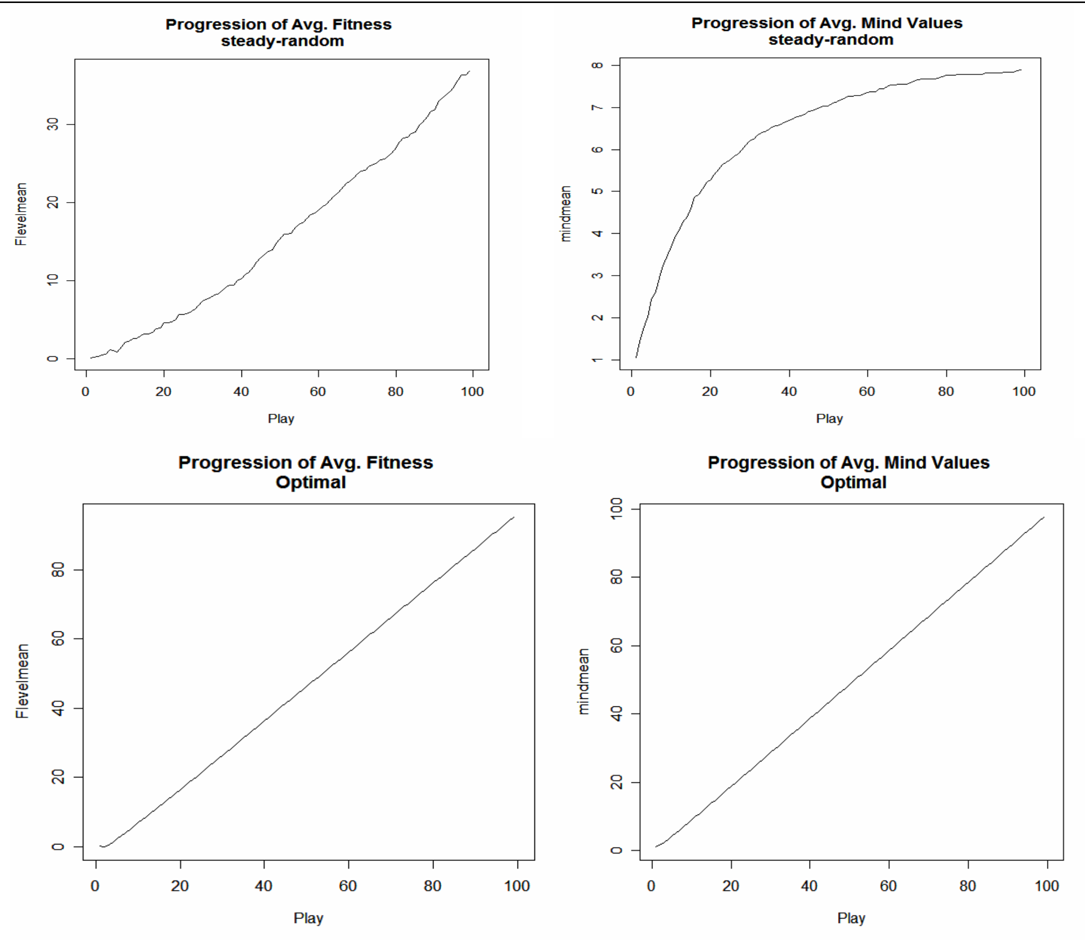

The top two illustrate the progression of a child's fitness and maturity, as measured by the number of times they've chosen mind over the course of 100 iterations of the Prisoner's Dilemma with a parent who randomly chooses actions while the bottom two are the results from interactions with a parent using tit-for-tat.

VI. References

[1] J. Logan, “A Game Theoretic and Genetic Algorithmic Approach to Modeling the Emergence of Mind in Early Child Development with Exposure to Semi-Developed Parents”.

[2] F. Happe “Theory of Mind and Self,” *Annals of the New York Academy of Sciences*, vol. 1001, Oct. 2003, pp 134.

[3] K. C. Pears, L. J. Moses, “Demographics, Parenting, and Theory of Mind in Preschool Children, “ *Social Development*, vol. 12, Feb. 2003, pp 1.

[4] J. Dunn, J. Brown, L. Beardsall, “Family Talk About Feeling States and Children’s Later Understandin of Others’ Emotions,” *Developmental Psychology*, vol. 27, May 1991, pp 448-455.

[5] L. Mayes, W. Miranker, “A Game Theoretic and Genetic Algorithmic Approach to Modeling the Emergence of Mind in Early Child Development,”

Cluster Analysis with Dynamically Restructuring Self-Organizing Maps

Daniel Holtmann-Rice

***Abstract*—Self-organizing maps (also called Kohonen networks) are a popular method of analyzing multidimensional data. In addition to compressing input data while preserving its topology, self-organizing maps can be used as a preliminary technique in cluster analysis. However, despite the fact that similar inputs remain close together in the output of the algorithm (suggesting possible clusters), no automatic segmentation of the data into discrete groups is provided. A variant of the SOM algorithm is proposed that dynamically clusters input data in an unsupervised fashion, automatically dividing the map into easily interpretable discrete submaps that correspond to clusters in the input data.**

***Index Terms*—knowledge acquisition, neural networks, self-organizing feature maps, cluster analysis**

I. Introduction

Humans are capable of performing unsupervised categorization tasks, in which they distinguish between and create categories around objects with which they have no prior experience. This process, called *category construction* in the literature on concepts and categorization (Murphy, [1]), is seen to occur quite frequently in children, and it is believed that children recognize objects as being in separate categories before they learn names for them (Merriman et al., [2]). Little is known about the precise mechanisms for how this is accomplished in humans, but being able to construct a system capable of simulating this behavior reliably would impact applications ranging from information storage and retrieval to object recognition and classification.

One presumably important mechanism in such a system is the analysis of multidimensional data, such as might be received from input sensors or from the feature-based analysis of text, images, sound, or other information. Specifically, the creation of discrete categories from a data set would seem to require some method of clustering the data, such that coherent groups are formed that maximize the similarity of data within a group while minimizing the similarity between groups. Such clustering is formally the assignment of labels to vectors in the input. The number of labels that are assigned is equal to the number of clusters in the data. To mimic cognitive capabilities, this must proceed in an unsupervised manner.

Thus it is necessary to discover algorithms capable of autonomously discovering clusters in a data set given minimal a priori information about the nature of the data set's distribution. Several statistical methods for clustering data exist and are widely used, however as these are not fully autonomous (requiring information regarding the expected number of clusters, and generally only capable of finding ellipsoidal clusters, cf. Costa and de Andrade Netto, [3]) they will not be reviewed here.

Models of neural systems look to be a more promising path. Many such models are capable of unsupervised learning and organization, and furthermore most are inherently amenable to neurobiological accounts of the processes involved (i.e., they are psychologically plausible). In particular, the self-organizing map algorithm, developed by Teuvo Kohonen, has several properties that make it well suited for analyzing large amounts of multidimensional data with the goal of discovering natural groupings within that data. There have been clustering techniques that make use of the SOM algorithm; these will be discussed in section III below.

After reviewing the relevant SOM-based approaches to cluster analysis and discussing some failed attempts at deriving autonomous cluster analysis tools, an algorithm is proposed that is capable of autonomously discovering clusters (including complex clusters with non-ellipsoidal shapes) by systematically adding and removing connections between units in the SOM, dynamically restructuring it in response to the underlying data distribution. In comparison with the traditional SOM algorithm, the proposed approach holds several advantages, including facilitated interpretation of the resulting map and better fit to the underlying data (as determined by visual inspection of the map).

II. The Self-Organizing Map Algorithm

A. *Capabilities of the self-organizing map algorithm*

Self-organizing maps (SOMs) are an effective tool in the analysis of multidimensional data. They are capable of converting high-dimensional data into a low-dimensional (often two-dimensional) representation that preserves the topological relations present in the primary data, in essence providing an estimation of the probability density function underlying the input data. SOMs have been widely used as tools to visualize high-dimensional data (Vesanto, [4]), and often act as guides in the exploratory phase of data mining (Vesanto and Alhoniemi, [5]). They have also been applied successfully in many natural language settings, having been shown to be capable of grouping words in a semantically meaningful way based on contextual information (Honkela et al., [6]). Furthermore, there is reason to believe that many of

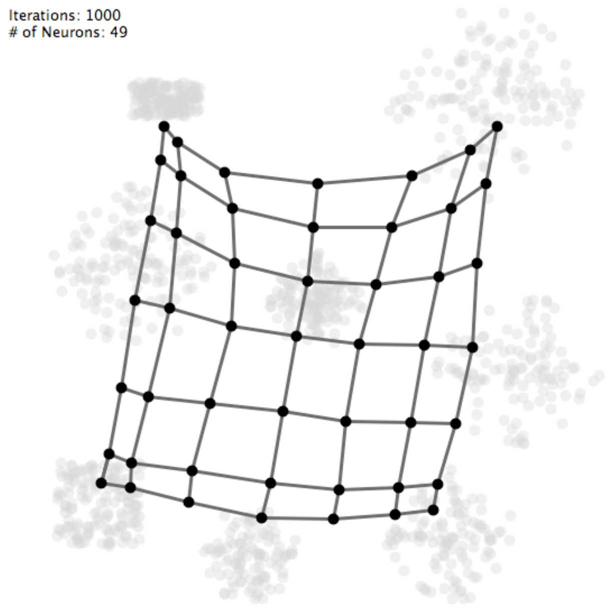

Fig. 1. The SOM algorithm with 49 neurons after 1000 iterations (well before convergence), on a two-dimensional input space. The grid-layout structure can be clearly seen. The black circles represent the neurons' locations in weight space, with links between the neurons represented as lines connecting them. Light-gray circles represent the weight-space locations of previously presented input data.

our own neurobiological subsystems may operate in ways similar to self-organizing maps. It has been shown (Ritter and Schulten, [7]) that SOM algorithms can successfully model sensory mappings and motor control functions, both of which are systems that the brain organizes topologically as well. Whether or not a SOM-based method for modeling aspects of the human conceptual system is feasible remains to be seen, but the place of SOM algorithms as effective knowledge representation devices is well established (Honkela, [8]).

B. *The algorithm*

A self-organizing map consists of a set of N neurons (also called units), each with l dimensional weight vectors that are initialized at random or from input data. Each neuron is "linked" to a number of other neurons (see Fig. 1) by a neighborhood relation that defines the structure of the map. (the choice of structure is rather flexible, a feature that will be exploited by the dynamic restructuring algorithm proposed in section IV). This linking is often done in such a way that the N neurons form a two-dimensional lattice – in this paper the SOM algorithm was implemented such that a two-dimensional grid of neurons was created, i.e. most neurons were linked to four other neurons (one in each direction, with the exception of neurons on the edges or corners of the grid). The set of neurons that a neuron is linked to is called its neighborhood.

The SOM algorithm proceeds iteratively, exposing the map to input data in the form of data vectors chosen with some probability from a data set. For each iteration, the algorithm proceeds as follows (refer to Haykin, [9], for a more in-depth analysis of the algorithm):

1. Select an input vector $\boldsymbol{x}$ at random from the data set.

2. Determine the "winning" neuron j whose weights are closest to the input vector in a Euclidean sense, i.e. the neuron whose weights $\boldsymbol{w}_j$ are closest to $\boldsymbol{x}$:

$$j = \arg\min_k \|x - w_k\|$$

3. Update the weights of neurons in the map in a fashion dependent upon their distance from neuron j. The distance $d_{j,i}$ between two neurons i and j is measured as the minimum number of links (as defined above) crossed when traversing the map from i to j. Let $h_{j,i}$ be a specified monotonic function that decreases with increasing d (in this paper the Gaussian function is used):

$$h_{j,i(x)} = \exp(-\frac{d_{j,i}^2}{2\sigma(t)^2})$$

where $\sigma(t)$ is an exponentially decreasing function that specifies the size of a neuron's topological neighborhood (intuitively, proportional to the extent of a neuron's influence over other neurons during an iteration). Weights for a neuron i are then updated according to the following function:

$$w_i(t+1) = w_i(t) + \eta(t) \cdot h_{j,i}(t) \cdot (x - w_j(t))$$

where $\eta(t)$ is a learning rate function that exponentially decreases with time.

This is continued for either a specified number of iterations or until a satisfactory level of convergence has been achieved.

III. Using the Self-Organizing Map Algorithm as a Tool for Cluster Analysis

The SOM algorithm does manage to maintain the topological relations of primary data quite well, resulting in a representation of the data where inputs that are close together (i.e. similar) in the primary data remain close together in the SOM. However, there is no immediate way of recognizing whether discrete clusters ("classes") of points are present in the data (and if so, how many) using solely the SOM algorithm. Furthermore, when presented with data that is not contiguous throughout weight space (as in Fig. 1, where the data is clearly composed of eight discrete regions), the SOM algorithm does a mediocre job of approximating the data distribution (Fig. 2), despite the fact that this is precisely the sort of data one would expect a clustering algorithm to have no difficulty with. Some neurons ("interpolating map units") converge to locations in between clusters of data points,

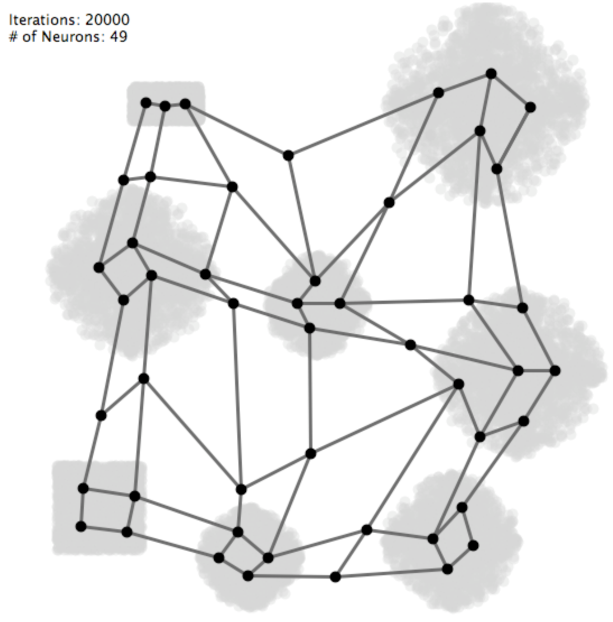

Fig. 2. Using the SOM algorithm, discontiguous clusters of data (grey) remain connected in the map. Many neurons are stranded in between clusters, leading to inaccurate coverage and inefficient use of neurons. Ideally the map should be broken into eight separate maps, each approximating one cluster of points.

leading to inaccurate coverage of the data and obscuring the borders between clusters (Vesanto and Alhoniemi, [5]). These two problems stand in the way of a simple approach to clustering using self-organizing maps (for a review of where we are heading, see Fig. 4).

Nonetheless, several cluster analysis techniques have been proposed that utilize the SOM algorithm in various ways. Vesanto and Alhoniemi ([5]) use a two-stage approach, where the SOM algorithm is run on a data set and then the resulting set of map units (not including those interpolating units that did not win frequently enough to be included) is analyzed using statistical clustering techniques. The underlying data vectors are associated with the map unit (neuron) closest to them and hence are clustered by association with the map units. While this is a useful technique from the perspective of reducing computational complexity (compared with clustering the underlying data directly), it also shares the problems of most statistical clustering techniques. It is not fully unsupervised, can only deal with ellipsoidal clusters, and despite avoiding the problem of interpolating map units (by not including them in the clustering), it does little to address the issue.

Costa and de Andrade Netto ([3]) also propose a two-stage clustering technique using the SOM algorithm. Their method involves running the SOM algorithm and then using image-processing techniques to analyze a visualization of the map. Clustering proceeds by segmenting the visualization, and labeling the map units based upon this segmentation. Unlike the Esa and Alhoniemi algorithm, Costa and de Andrade Netto's method is truly unsupervised, and is able to generate complex-shaped clusters. However, it too does not address the issue of interpolating units directly.

In order to both address the issue of interpolating units and to develop a simpler technique for creating easily interpretable clusters from SOM data, it is our intention to modify the SOM algorithm so that some of the links between units in the map are systematically weakened or removed, in such a way that smaller "submaps" emerge, each covering a contiguous region of input space and representing a cluster of points within the data.

IV. Modifications to the Algorithm

A. Unsuccessful Attempts

To gain insight, we first discuss several "naive" attempts at modifying the algorithm that did not succeed.

1) The "Strain" Method

The first attempted modification was to use the length ("strain") of the links between neurons as a way of weeding out those links that were connecting two neurons from distinct clusters of data. In this modification, each neuron keeps track of the average length of its links (i.e. its average distance from its neighbor neurons). If the ratio between the length of a link to a neuron and the average length of other links connecting to that neuron is above some threshold value, then the link is removed.

The problem with this method is that long links tend to raise the average length of a neuron's links, and thus a neuron with more than one long link all of which should be removed doesn't remove them because their ratio to the average isn't above the threshold value. Comparisons involving variance or standard deviation fail for the same reason. Using the difference between a link's length and the average link length for a neuron doesn't scale – if the neurons are spread out, link size differences will naturally be larger (since one can expect the link sizes to be more varied) than when the neurons are closer together (assuming the neurons are spread out evenly), and this shouldn't result in removal of links.

2) The "Pull" Method

The second attempted modification kept track of the average direction of a neuron's closest neighbors over time, and used this information to penalize links to neurons trying to pull it in an opposing direction. This was calculated as the weighted sum of the "direction vectors" for each link connected to it (the position of the neighboring neuron minus the position of the neuron in weight space), with each link's direction weighted by the inverse of its length (using a Gaussian function was also tried, but this proved equally unsuccessful). This vector (the "pull vector") was used to weed out links to neighbors that were trying to move the neuron in a direction opposing the pull vector. For each link, the dot product of its direction (the position of the neighbor minus the position of the neuron) with the pull vector was calculated, and if this was below some threshold value, the link was removed. However, the method of calculating the pull vector was inadequate – the direction vectors of links were weighted by the inverse of their length in order to favor shorter links, but this didn't seem to scale when neurons were farther apart (since the difference

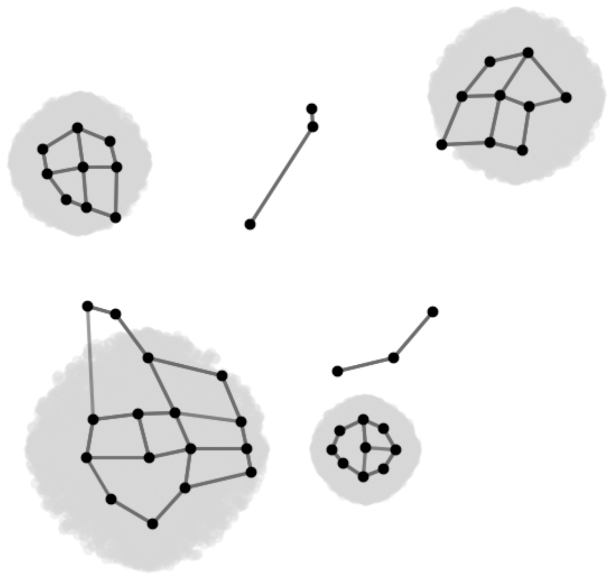

Fig. 3. The "Reward" method as used on a data set containing four clusters. As can be seen, while it successfully creates a submap for each cluster, it does not deal with interpolating units, and has converged to a less than desirable state.

between the inverses of the lengths became smaller) and thus the pull vector became skewed. To fix this, a non-arbitrary way of scaling the inverse function (or Gaussian function) used to weight the directions would need to be found.

3) The "Reward" Method

A slightly more successful method involved using a reward system for links that connect two neurons that consistently have input vectors fall between them in weight space. Instead of finding only the closest neuron to the input vector, the two closest are found, and if there is a connection between them, the "strength" of this connection is set to 1. Then the strength of all the other links from the winning neuron are decreased by some small amount. The strength of each link ξ is used during the weight modification stage of the algorithm to decrease the effect of links with lower strengths:

$$w_i(t+1) = w_i(t) + \xi_i(t) \cdot \eta(t) \cdot h_{i,j}(t) \cdot (x - w_j(t))$$

Over time, the strength of a link may decrease to 0, and thus is effectively removed.

Results of this method can be seen in Fig. 3. While this succeeds in breaking the map down into smaller pieces that partially capture the discrete regions present in the input data, the accuracy (the number of neurons stranded between clusters and the general fit to the underlying data) is only improved very slightly, if at all. The problem with this approach is that it takes a long time for many of the links to start decreasing in strength, and by the time they do, the distance function *h* has decreased to the point where neurons don't affect their neighbors enough to move them very far in weight space. Thus neurons get stranded in between the data clusters.

B. The Proposed Method (The Dynamic SOM Algorithm)

1) Motivating Factors

Several issues had to be addressed in order to overcome the obstacles encountered during the first three "naïve" attempts at modifying the algorithm.

1. Some method to deal with interpolating units (units that get stranded between clusters) is necessary
2. The map should not be allowed to converge prematurely
3. Link modification should not take place until the map has converged substantially
4. If a method for removing links is present, a method for adding links needs to be included as well
5. Map units should not have links of wildly differing lengths ("strains")

A robust and simple method of dealing with interpolating units is to kill neurons that have gone too many iterations without winning. This simply involves having each neuron store an "age" property, that is incremented by unity every iteration and reset to zero if a neuron is the winning neuron for that iteration. This method was originally biologically inspired (though subsequent research indicated it was by no means a new concept, as Vesanto and Alhoniemi make use of essentially the same idea to cull interpolating units). During development of the human motor system, many more motor neurons are created than will actually used by the developing child. While still in the womb, motor neurons undergo Hebbian competition, and neurons that do not get activated with enough frequency eventually die off (Kandel et al., [10]).

In order to address the issue of premature convergence, the learning rate ($\eta(t)$) and neighborhood topology ($\sigma(t)$) functions are modified such that they never fully reach zero. This ensures that the neurons never completely converge, and can still adapt to changing input (though not very much). In light of the motivation for the current algorithm (mimicking the human ability to categorize in an unsupervised manner), complete convergence, and hence a complete loss of plasticity, seems undesirable.

Any link modification techniques are meaningless until the map has at least ordered itself (topologically oriented itself such that there are a reduced number of intersecting links) and converged to a point where metrics such as link strain or neuron age have some meaningful relation to the underlying data (i.e., can be used as reliable indicators of how well the map is approximating the data's distribution). Thus a "minimum convergence" threshold is specified, and link and neuron modification only takes place when the last iteration's total "change" (the sum of the distances traveled by the neurons in weight space) is less than the threshold value. Until this point the algorithm proceeds identically to the standard SOM algorithm.

If links were only allowed to be removed, then the map would become rather sparse, and this would inhibit clear-cut analysis of clusters as well as undermining the intuitive appeal of using links as a representation for "connectedness" within the map (i.e., neurons and the categories they represent are more similar the more connections there are between them).

Thus a method for adding links is included: instead of only computing the winning neuron, the winning neuron and the second closest neuron are computed. If a link exists between the neurons, this link's age is reset to zero. If no such link exists, it is created. Every time a neuron wins an iteration, the "age" properties of the links connected to it are incremented (with the exception of the link between the winning neuron and the second closest neuron, which is reset). If a link's age is too great, then the link is removed. This method of link addition and removal is extremely similar to that employed by the "Growing Neural Gas" algorithm originally developed by Fritzke ([11]), and is equivalent to the "Reward" method discussed earlier (which however dealt only with link removal).

Finally, links that are significantly longer than others on the neurons they connect to should be removed to speed the convergence process (in general, these links will be removed by the aging process mentioned above, but removing them proactively makes the convergence process faster). To determine whether a link from a given neuron should be affected, the links from that neuron are first sorted by their length. Then, this sorted list is traversed in order, and each link is compared to the link preceding it in the list. If the ratio between them is greater than some threshold value, the link and all subsequent links in the list (i.e. the link and all all links longer than it) are "weakened" by some amount, while links in the list previous to the link being tested are "strengthened" by some amount. If a link's strength property reaches zero (i.e. it has been weakened several times in a row) then the link is removed. Any neurons that don't have any links after this process are also removed.

2) *A Summary of the Dynamic SOM Algorithm*

1. Select an input vector ***x*** at random from the data set.
2. Determine the "winning" neuron *j* whose weights are closest to the input vector in a Euclidean sense, as well as the "second best" neuron k whose weights are second-closest to the input vector.
3. If the map is sufficiently converged (i.e. the total distance moved by all the neurons in the map over the previous iteration is below some threshold):
    a. Age all links connected to j by 1 and reset j's age to zero.
    b. Check to see if a link exists between j and k. If so, reset its age to zero, and if not, create it.
4. The conventional SOM update step occurs, and neurons within the topological neighborhood of the winning neuron are moved closer to ***x***.
5. If the map is sufficiently converged (using the same criteria as above), for each neuron:
    a. Sort its links by length.
    b. Find the link whose ratio to an adjacent link is greater than some threshold.
    c. Weaken that link and all links longer than it.
    d. Remove links whose strength is zero.
    e. Remove links that are older than some threshold.
    f. If the neuron is older than some threshold or has no links attached to it, kill it.
    g. Age the neuron.

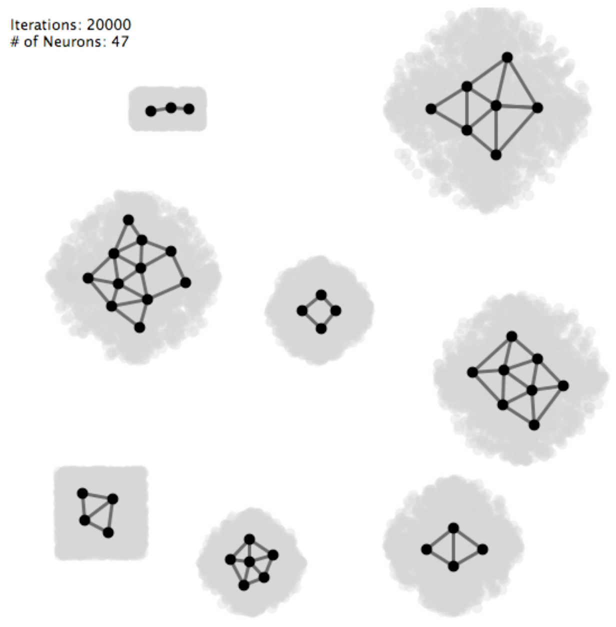

Fig. 4. The dynamic SOM algorithm breaks into 8 separate maps, one for each cluster present in the input data. Two neurons die in the process.

V. Results and Discussion

A. *Comparison with the Traditional SOM Algorithm*

Fig. 4 shows the same data set from Fig. 1 as analyzed by the dynamic SOM algorithm. The modified SOM algorithm does a substantially better job of staying true to the distribution of the underlying data as a result of its flexible structure. While this is difficult to quantify, it is readily apparent from visual inspection. As can be seen, there are no more interpolating map units, no connections between clusters, and link sizes are all relatively uniform. Many links between neurons have been added, leading to submaps that are extensively interconnected. Two neurons that didn't make it to the "safety" of a cluster before they grew too old were removed entirely.

The algorithm is also capable of clustering complex shapes. The appendix to this paper contains several comparisons between the regular SOM algorithm and the dynamic algorithm, some of which demonstrate *the ability of the dynamic algorithm to cluster non-linearly separable collections of data*.

Based on experience with the algorithm, it appears that approximately 5-15% of neurons die during the analysis of a given input data set. Lowering this number (ideally all neurons should survive to prevent information loss) remains a task for future work.

B. *Comparison with the Human Conceptual System*

Despite the dynamic SOM algorithm's flexibility, it is difficult to imagine it acting as a real-time model of human category construction tasks (if only due to efficiency concerns). However, it shares several properties with the conceptual system that are worth noting. These are (explanations to follow):

1. It functions as a cross between exemplar and prototype models of category representation.
2. Active "perception" in a specific area of weight-space changes representation of that area of weight-space.
3. It functions by viewing only one piece of input data at a time, much as we do (with selective attention).

1. Two approaches to category representation exist in the concepts and categories literature (Murphy, [1]). The "exemplar view" holds that we store every memory of things we've encountered that belong to a certain category. When we categorize a novel object, we compare that object to every exemplar we have stored in memory, and choose the most similar exemplars for use in categorizing the object. The opposing view is that we "average" our interactions with category members to arrive at an "idealized" category member – a prototypical member of the category. The SOM algorithm represents clusters using what could be viewed as a set of multiple prototypes. This is not as memory intensive as the exemplar approach, and not as limiting from a representational standpoint as the prototype approach.

2. It is reasonable to assume that our representation of a concept only changes when we interact with or think about instances of that concept (or very similar concepts). This is similar to the SOM algorithm, since there is a limit to the influence of an input vector – it only affects the neurons closest to it.

3. When we interact with objects in the world, we interact with them generally one at a time. Thus, whatever system we have for learning and organizing our conceptual knowledge must operate on minimal input, i.e., it can function without knowing a priori the size, distribution, and frequency of a category – it can learn based on seeing only one instance of that category at a time. The SOM algorithm operates on similar principles.

Finally, one aspect of the SOM algorithm as implemented here that differs substantially from human conceptual experience is the lack of temporal continuity with respect to input. When we walk into a room, we are faced with the same set of objects for an extended period of time. This is not the case with the SOM algorithm, where input data is selected randomly, and there is no reliable relation between one input vector and the next.

C. Remaining Problems and Future Work

Several problems with the dynamic SOM algorithm remain. Clusters must be spaced rather far apart in order for the algorithm to detect them and not treat them as contiguous regions of input data. There is an inverse relationship between the number of neurons in the map and the minimum separation between clusters that must be present in order for clusters to be accurately identified – more neurons in the map makes the spacing between neurons smaller, which means links between clusters are less likely to be activated.

The algorithm is also slow. Due to the similarity between this algorithm and the growing neural gas algorithm, it would thus be desirable to do a direct comparison between the two to see which converges faster.

Finally, the algorithm has not yet been tested on real-world data. It remains to be seen whether it can accurately and meaningfully detect clusters in multidimensional real-world data, however the preliminary results from synthetic data are promising.

References

[1] Murphy, G. *The Big Book of Concepts*, Cambridge, MA: MIT Press, 2002.

[2] Merriman, W. E., Schuster, J. M., and Hager, L. (1991) Are names ever mapped onto pre-existing categories. *Journal of Experimental Psychology: General*, *120*, 288-300.

[3] Costa, J.A.F.; de Andrade Netto, M.L., (1999) Cluster analysis using self-organizing maps and image processing techniques. *IEEE International Conference on Systems, Man, and Cybernetics, 1999*, vol. 5, pp. 367-372.

[4] Vesanto, J. (1999) SOM-based data visualization methods. *Intelligent Data Analysis*, vol. 3, pp. 111–126.

[5] Vesanto, J. and Alhoniemi, E. (2000) Clustering of the Self-Organizing Map. *IEEE Transactions on Neural Networks*, vol. 11, no. 3, pp. 586-600.

[6] Honkela, T., Pulkki, V., & Kohonen, T. (1995) Contextual Relations of Words in Grimm Tales Analyzed by Self-Organizing Map. *Proceedings of ICANN-95, International Conference on Artificial Neural Networks*, vol. 2, F. Fogelman-Soulié and P. Gallinari (eds.), EC2 et Cie, Paris, pp. 3-7.

[7] Ritter, H. J. and Schulten, K. (1988) Kohonen's self-organizing maps: Exploring their computational capabilities, In: *Proc. IEEE Int. Conf. Neural Network, ICNN-88*, San Diego, CA, pp. 109-116.

[8] Honkela T. (2000) Adaptive and Holistic Knowledge Representations Using Self-Organizing Maps. *Proceedings of IIP'2000, International Conference on Intelligent Information Processing*, Z. Shi, B. Faltings and M. Musen (eds.), Beijing, China, August 21-25, 2000, pp. 81-86.

[9] S. Haykin, *Neural networks: A comprehensive foundation*, Upper Saddle River, NJ: Prentice-Hall, 1994.

[10] Kandel, E. R., Schwartz, J. H., Jessell, T. M. *Principles of Neural Science*, 4th Edition, Chicago, IL: The Unviersity of Chicago Press, 2000.

[11] Fritzke, B. (1995) A Growing Neural Gas Network Learns Topologies, in: Tesauro, G., Touretzky, D. S., Leen, T. K. (Eds.): *Advances in Neural Information Processing Systems 7*, MIT Press, 625-632.

VI. Appendix: A Graphical Comparison Between Regular SOM and Dynamic SOM Algorithms

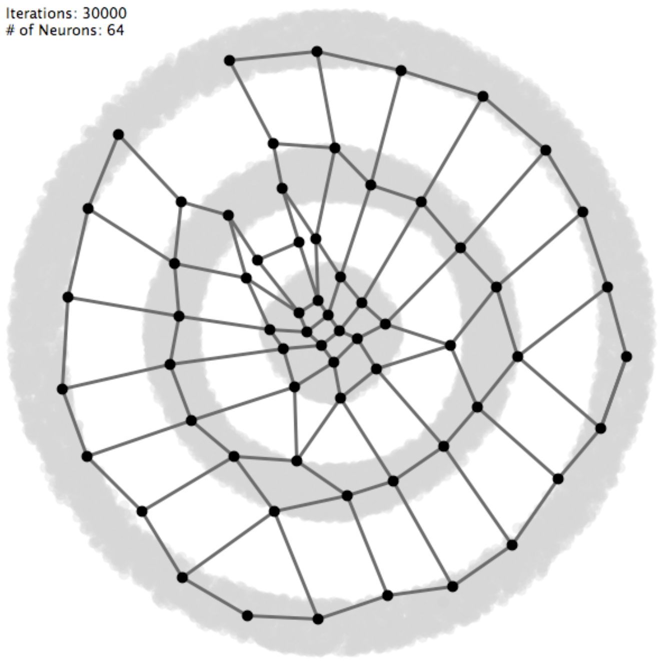

Fig. 5(a) The classical SOM algorithm's analysis of input data consisting of concentric rings. Not the unclosed gap as a result of the grid shape being stretched to fit around the rings.

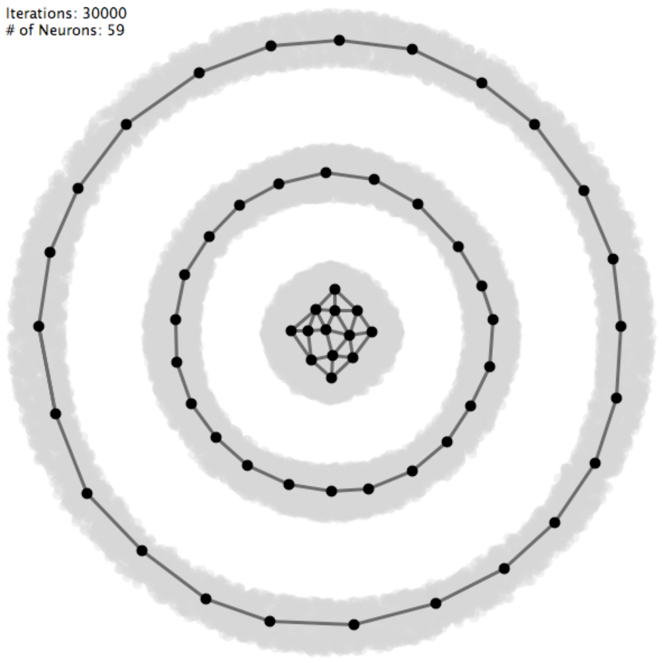

Fig. 5(b) The dynamic SOM algorithm's analysis of the same data. Distribution of neurons is very uniform, and there are no links between the rings. Six neurons died.

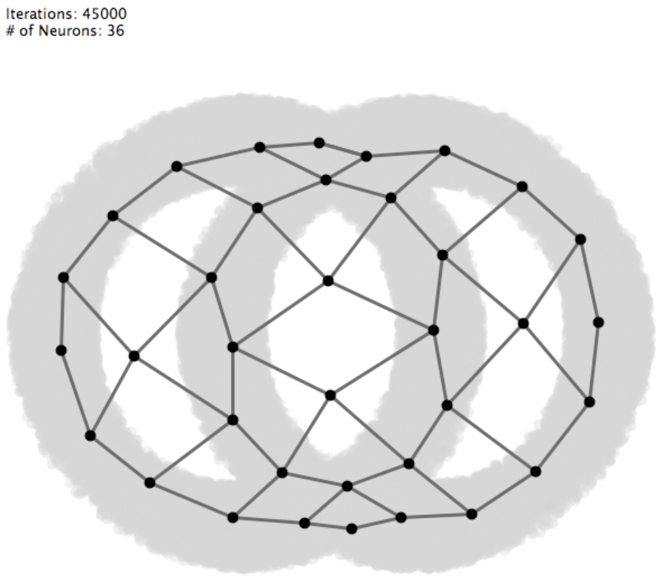

Fig. 6(a) The classical algorithm's analysis of two interlocking rings. There are interpolating neurons in all three "holes", and this inefficient use of neurons makes the distribution of neurons along the rings less dense.

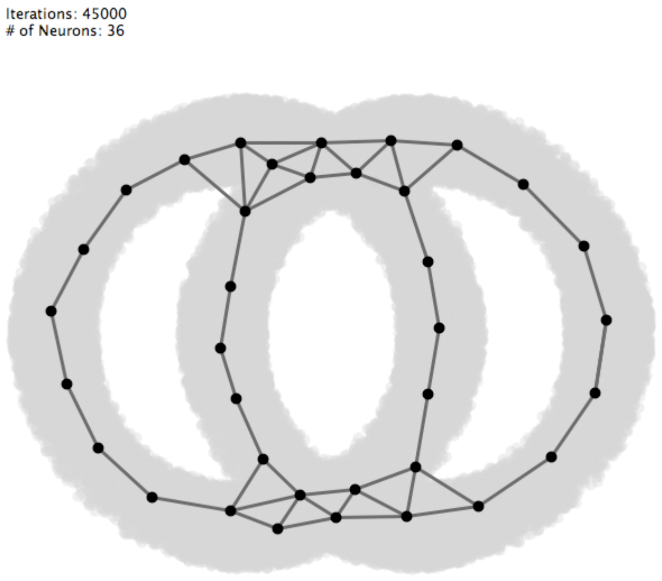

Fig. 6(b) The dynamic SOM algorithm's analysis of the same data. No neurons died.

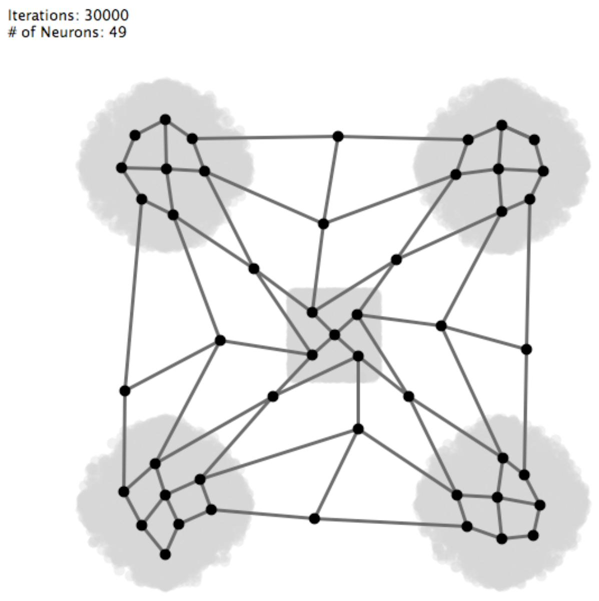

Fig. 7(a) The classical algorithm's analysis of a five-cluster input data set. Due to the symmetrical nature of the data, the presence of interpolating map units is particularly prominent.

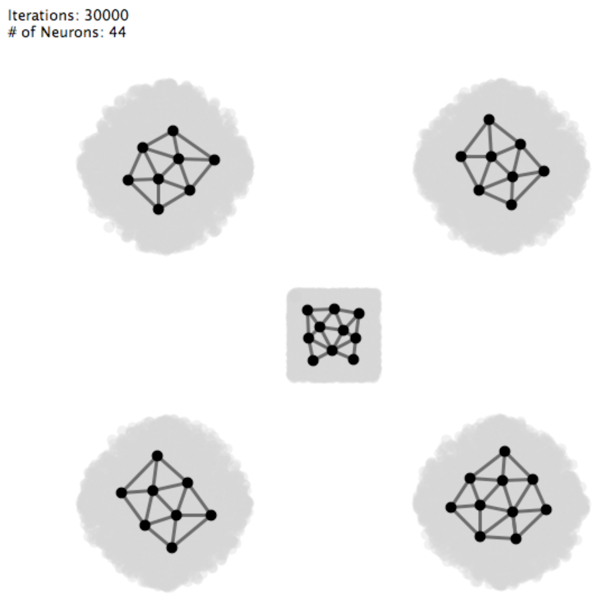

Fig. 7(b) The dynamic SOM algorithm's analysis of the same data. Five neurons died.

Dimensionality Reduction via Self-Organizing Feature Maps for Collaborative Filtering

Andrew R. Pariser

Abstract—**With customer preference databases growing to colossal sizes, collaborative filtering algorithms run into scalability concerns. By reducing the dimensionality of the input space, we ease the demands of predicting users' tastes for films. A movie-to-movie correlation and distance metric are used to decompose the user-movie rating data into two different movie graphs. Using a Kohonen self-organizing map (SOM), the product space can be divided into meaningful clusters centered on the neurons whose weight vectors are nearest the product weights. The SOM –derived clustering is analyzed via a Principal Components Analysis of the data. The clusterings are then evaluated for their effectiveness via quantitative and qualitative observations on the meaningfulness of the groupings of the films.**

***Index Terms*—Clustering methods, Collaborative filtering, Karhunen-Loeve transforms, Movies, Neural network applications, Self-organizing feature maps**

I. Introduction

COLLABORATIVE filtering, the automated process of making predictions about a user's interests given data collected on customers' prior preferences, has become an increasingly relevant problem. Mindful companies are cataloging their customers' every move, hoping to uncover meaningful trends that help refocus product selection and marketing. Collaborative filtering need not only be seen as an aid to the seller, however; customers, who are more regularly inundated by an increasingly complicated market with thousands of slightly differentiated products, benefit highly from individualized product suggestions.

The substantial size of the customer preference databases (the inputs for collaborative filtering) makes the problem of individualizing the recommendation process even more difficult [6]. Collaborative filtering techniques generally fall into two groups by the type of approach, either memory-based or model-based algorithms. The former make determinations according to an analysis of the entire dataset whereas the latter fine-tune a user-specific model designed to capture an individual's relationship to the entire product space. Each approach presents difficulties when scalability is a concern [6].

A. Pariser is a senior at Yale University, expecting graduation with a BS in May of 2007 for a Physics and Applied Mathematics double major, (e-mail: andrew.pariser@yale.edu).

This paper proposes dimensionality reduction via product clustering as a solution to the problem of scalability. The *product space*—here, the set of all films—when partitioned, becomes more manageable for calculations. In the same way that the human brain generates classification schema to aid in comprehending the world [1], collaborative filtering algorithms can consider a user's relationship to these categories (instead of looking at the user's relationship to each individual item independently) [5].

The partitioning of the product space is accomplished by training a Kohonen self-organizing map on relational film data. The resulting clusters are analyzed and then graphed via a principal components analysis. It is hard to quantitatively measure the partitions that emerge, though data on the films' genres, directors contribute to a qualitative assessment of the clustering algorithm.

The clusters derived from the self-organizing map are by no means perfect, though the similarity between the films in each partition is no accident. In almost every partitioning of the films, movies end up in the same clusters as their sequels (with the noted exception of the Harry Potter franchise, where the third and fourth films are markedly different than the first and second, both sets of which are grouped in different clusters). Most clusters seem to exhibit some property that differentiates the films in the particular group from the entire set of all movies being considered, be it genre, budget, director style, or some more subjective quality.

Indeed, the quality of the partitions is impressive considering the amount of data that is aggregated to arrive at the results. This suggests that SOM algorithms like this one may provide the key to developing collaborative filtering systems in the face of increasing scalability concerns.

II. The Netflix Prize™ Data

Netflix provides the following as description of its data:

"The movie rating files contain over 100 million ratings from

480 thousand randomly-chosen, anonymous Netflix customers over 17 thousand movie titles. The data were collected between October, 1998 and December, 2005 and reflect the distribution of all ratings received during this period. The ratings are on a scale from 1 to 5 (integral) stars. To protect customer privacy, each customer id has been replaced with a randomly-assigned id. The date of each rating and the title and year of release for each movie id are also provided."

The five hundred most rated movies were extracted from this dataset for the tests that follow, representing a meaningful portion of the entire population of ratings while keeping computation time reasonable. These films comprise the *product space* of this research.

III. Taste Profile Decomposition

A. Overview

It is difficult to find a basis on which one can partition the set of viewer-movie rating pairs. Instead, one would intuitively think to create groupings among either the set of movies or the set of users. A cluster from the set of users would hopefully contain customers who would rank movies similarly. Likewise, a cluster from the set of movies would ideally collect all titles which will probably receive the same ratings across all users.

The goal of this first step is to transform the viewer-movie rating pairs into data that relate the films via some calculation on collective ratings data, simplifying hundreds of user ratings for two films into one value.

B. Movie-Movie Metrics

In order to transform the user-movie rating pairs into a relational graph of movies, we must aggregate the user data via some metric that relates two movies. We consider two such measures, a correlation metric and a distance metric.

Let $U(m)$ represent the set of all users who have rated movie m. We define $U(m,n) = U(m) \cap U(n)$ as the set of users who have rated both movies m and n. Using the variable u to represent a user, we define $r_m(u)$, μ_m, and σ_m as the rating user u gives movie m, the mean rating for movie m, and the standard deviation of all users' ratings for movie m, respectively. We then consider the functions

$$\rho_{mn} = (\sigma_m \sigma_n)^{-1/2} \sum_{u \in U(m,n)} (r_m(u) - \mu_m)(r_n(u) - \mu_n) \tag{1}$$

and

$$d_{mn} = \sum_{u \in U(m,n)} (r_m(u) - r_n(u))^2 \tag{2}$$

where (1) represents a measure of correlation and (2) a measure of distance between m and n.

The resulting data from equations (1) and (2) are then normalized so that $-1 \leq \rho_{mn} \leq 1$ and $0 \leq d_{mn} \leq 1$. To sharpen the metrics and to aid in providing clearer boundaries on which to cluster the graphs, we exponentiate the results of the two formulae above, obtaining

$$\rho'_{mn} = \exp(-\rho_{mn}) \tag{3}$$

and

$$d'_{mn} = \exp(-d_{mn}) . \tag{4}$$

The bounds on (3) and (4) are $0.368 \leq \rho'_{mn} \leq 2.718$ and $0.368 \leq d'_{\mathrm{mn}} \leq 1$, and are determined by transforming the bounds on (1) and (2).

The values from (3) and (4) are compiled into two matrices, $\mathrm{P} = (\rho'_{mn})$ and $D = (d'_{mn})$.The columns of these two matrices, which we denote P_m and D_m respectively, correspond to vectors in the *input space* of the system. The elements in each vector define the particular movie in relation to the other films via the relational metrics in (3) and (4).

That the 500 most rated Netflix films were extracted from all movies provided in the dataset proved useful not only for computation time. Equations (1) and (2), which relate two films, depend upon having a non-empty intersection $U(m,n) = U(m) \cap U(n)$. It would be unclear how to speak of a "correlation" or "distance" between two products if one could not find a common subset of users who have provided taste profiles on both products. Thankfully, when limiting the data to the top 500 most rated films, the size of the intersection, $|U(m,n)|$, is strictly positive and thus Equations (1) – (4) are always defined.

An introductory analysis of the 500 most rated Netflix films is compiled in Appendix A. It includes lists of the ten most rated films, the ten films with highest and lowest ratings, and the ten films with highest and lowest variance in their ratings. Additionally, insight into the metrics of Equations (1) and (2) is provided by listing the ten most and least correlated films, as well as the ten most and least distant films.

IV. Clustering via Self-Organizing Map

A. Definition and Motivation

Self-organizing maps (SOMs) distinguish features from an input space by forming topographical representations of their input patterns. Using competitive learning, "winning" neurons (and their neighbors) adjust their weight vectors to move closer to presented inputs (the columns of P and D) in synaptic weight space. After a convergence phase, the resulting neuron assembly exhibits important properties of the input space [2]:

1. The feature map, as represented by the set of synaptic weight vectors, approximates the entire input space
2. The feature map is *topologically ordered*. That is, the spatial locations of the neurons represent a particular feature or subset of the input space.
3. The neuron density of the resulting feature map mimics the probability density of the input space.
4. As a conclusion of the previous three properties, a self-organizing map is able to select a set of best features for approximating an underlying distribution.

Given these four properties, one can easily assign clusters to movies from a particular SOM network: for each movie in the input space, it belongs in the cluster corresponding to the neuron nearest it in weight space.

B. *Specification of SOM model and parameters*

Two SOMs are trained on each of the input spaces defined by the sets of column vectors $\{P_m\}$ and $\{D_m\}$, one with N neurons, both for $N = 10$ and $N = 30$. The output, therefore, corresponds to four different clusterings, one for ten clusters of each input space and the other of thirty clusters of each input space.

In these four clusterings, the synaptic weight space for each network is $[0.368, 2.718]^{500}$ and $[0.368, 1]^{500}$, for P_m and D_m, respectively. The initial synaptic weights for the fifty neurons are chosen randomly from the sets $\{P_m\}$ and $\{D_m\}$.

At each iteration n of the network training phase, an input vector $\mathbf{x}(n)$ is presented to the network, where the input vector is given by a column vector of P or D, allof which are presented in a randomly permuted order in each training epoch. Competitive learning is used such that a best-matching (winning) neuron $i(\mathbf{x})$ is chosen according to the minimum-distance criterion:

$$i(\mathbf{x}) = \underset{j\in\{1,2,\ldots,N\}}{\arg\min} \left\| \mathbf{x}(n) - \mathbf{w}_j \right\|$$

The winning neuron moves its weights in the direction of the input presentation $\mathbf{x}$ according to the update formula

$$\mathbf{w}_j(n+1) = \mathbf{w}_j(n) + \eta(n)\, h_{j,i(\mathbf{x})}(n)\,(\mathbf{x}(n) - \mathbf{w}_j(n)),$$

where the learning rate function is defined by

$$\eta(n) = \eta_0 \exp(-n/\tau),$$

and the neighborhood function is defined to be the Kroniker delta function

$$h_{i,j}(n) = \delta_{ij} = \begin{cases} 1 & \text{if } i = j \\ 0 & \text{otherwise} \end{cases}.$$

Choosing the particular parameters for these functions affects the speed and accuracy of the network training algorithm. Making $\eta(n)$ ineffective by starting η_0 too low may trap the network in local minima, whereas choosing η_0 too high can cause the network to exhibit unfortunate oscillatory behavior. Similarly, these same effects can be achieved by changing the exponential decay of $\eta(n)$ improperly; the network may overshoot optimal regions when τ set too high, whereas, if τ is set too low, the network will converge very slowly if at all.

C. *Choosing Network Training Parameters*

The learning rate parameters $\eta_0 = 0.01$ and $\tau = 1000$ are suggested by Haykin [2]. In selecting these parameters, one would hope to find the minimum value for the total self organizing map error as a function of the network's weights $\mathbf{W}$ given by

$$\mathcal{E}(\mathbf{W}) \equiv \text{total\_net\_error}\,(\mathbf{W}) = \sum_{j=1}^{500} \left\| \mathbf{W}_{i(\mathbf{x}_j)} - \mathbf{x}_j \right\|^2 . \quad (5)$$

Here, the input vectors $\{\mathbf{x}_1, \ldots, \mathbf{x}_{500}\}$ correspond to the column vectors $\{P_m\}$ and $\{D_m\}$ as the case may be, and the term $\mathbf{W}_{i(\mathbf{x}_j)}$ symbolizes the weight vector of the best-matching (winning) neuron $i(\mathbf{x}_j)$ for the given input vector $\mathbf{x}_j$. Once each network has been sufficiently trained, this value in (5) no longer decreases.

For each matrix and each number of output clusters, multiple values for each of the network training parameters η_0 and τ were compared according to their ability to minimize this error $\mathcal{E}(\mathbf{w})$.

Tables 1 and 2 show results from these calculations. Shaded rows in each table correspond to parameter choices producing the lowest final values of the error $\mathcal{E}$ found. The values for η_0 and τ for the actual training of each network were read directly from these shaded rows.

Table 1 – Optimal Parameters, P-Network Training

10 Clusters, P			30 Clusters, P		
$\mathcal{E}$	η_0	τ	$\mathcal{E}$	η_0	τ
0.9389	0.1	250	0.8856	0.1	250
0.9314	0.1	500	0.8683	0.1	500
0.9302	0.1	750	0.8606	0.1	750
0.9299	0.1	1000	0.8578	0.1	1000
0.9334	0.2	250	0.8656	0.2	250
0.9267	0.2	500	0.8563	0.2	500
0.9264	0.2	750	0.8486	0.2	750
0.9238	0.2	1000	0.8509	0.2	1000
0.9304	0.3	250	0.8593	0.3	250
0.9245	0.3	500	0.8489	0.3	500
0.9259	0.3	750	0.8429	0.3	750
0.9227	0.3	1000	0.8439	0.3	1000

Table 2 – Optimal Parameters, D-Network Training

10 Clusters, D			30 Clusters, D		
$\mathcal{E}$	η_0	τ	$\mathcal{E}$	η_0	τ
0.9389	0.1	250	0.8856	0.1	250
0.9314	0.1	500	0.8683	0.1	500
0.9302	0.1	750	0.8606	0.1	750
0.9299	0.1	1000	0.8578	0.1	1000
0.9334	0.2	250	0.8656	0.2	250
0.9267	0.2	500	0.8563	0.2	500
0.9264	0.2	750	0.8486	0.2	750
0.9238	0.2	1000	0.8509	0.2	1000
0.9304	0.3	250	0.8593	0.3	250
0.9245	0.3	500	0.8489	0.3	500
0.9259	0.3	750	0.8429	0.3	750
0.9227	0.3	1000	0.8439	0.3	1000

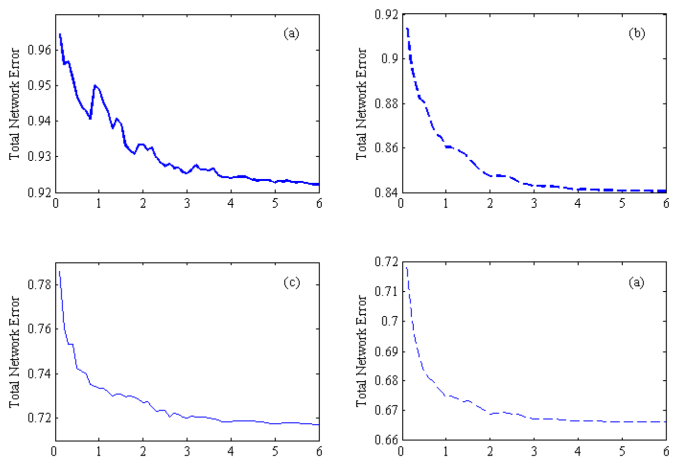

Figure 1 – Training Error vs. Number of Epochs

Bold lines in Figures (1a) and (1b) correspond to networks trained on P, whereas the regular lines of Figures (1c) and (1d) show the error for networks trained on *D*. The solid lines in Figures (1a) and (1c) are ten neuron networks; dashed lines in Figures (1b) and (1d) are thirty neuron networks.

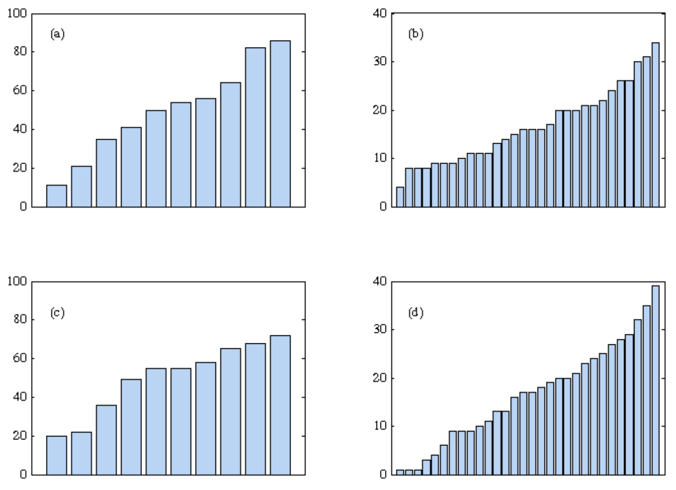

Figure 2 – Cluster Sizes

These four charts indicate (in increasing order) the size distribution of each of the four networks. Figures (2a) and (2c) are the ten neuron cases and Figures (2b) and (2d) are the thirty neuron cases for the P and *D* matrices, respectively.

D. Training Phase

The self organizing map converged on its ultimate synaptic weight locations in no more than six training epochs, with the presentation of the entire input space in randomly permuted order per epoch. Figure 1 shows the network training error for each of the four ways of clustering the graphs.

Figure 2 shows the cluster sizes of each the clusterings that result from each trained SOM.

V. Principle Components Analysis

A. Definition and Motivation

A principal components analysis (PCA) of a dataset is a statistical operation that shrinks multidimensional data into lower dimensions. PCA is the linear transformation of any multidimensional data **X** into a subspace **Y** for maintaining the largest variance. The data **Y** is just a projection of **X** onto the *m* eigenvectors of **X** that have the largest eigenvectors. The transformation, also called the discrete Karhunen-Loeve transform, is used for pattern recognition and minimizes data reconstruction error under the L^2 norm [3]. In our case, we reduce 500-dimensional data P and *D* into two-dimensional so that we may visualize the films' locations.

B. Applying PCA to Movie-Movie Interaction Data

One can transform the data P or *D* into a reduced subspace by repetitively subtracting the projection of the data on the first *l* eigenvalues from P or *D*, respectively, and then calculating the projection of this residual on the $(l + 1)^{th}$ eigenvector.

Choosing the output to be either two- or three-dimensional data allows complicated data in P or *D* to be visualized. These reduced dimension points allow us not only to visualize movies but also to visualize clusters on these movies. Ideally, clusters should contain points that are not very distant after a PCA transformation.

Figures 3 through 6 show the different clusters resulting from the SOM algorithm for each of the four scenarios, as plotted on two-dimensional PCA coordinates.

Indeed, we note that the films which are in the same clusters are near each other in the reduced dimensional space generated by the PCA analysis. And, furthermore, there are few overlapping lines from different clusterings, which is consistent with the desire for clusterings to partition the input space into regions that are both contiguous and disjoint possible.

Along these lines, we can identify some regions that may be problematic, specifically in the lower left quadrant of the P data in Figures 3 and 4.

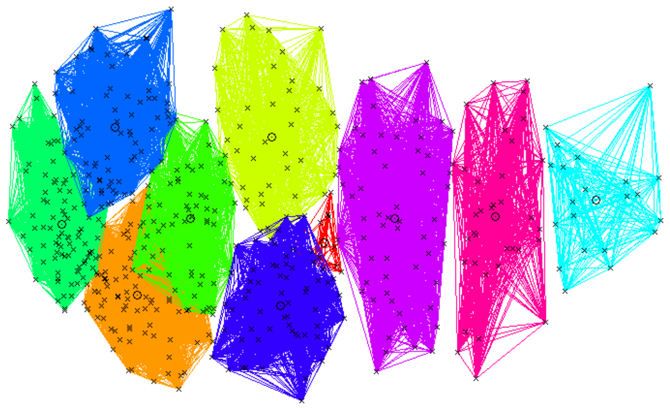

Figure 3 – Ten-Clustering of P Data

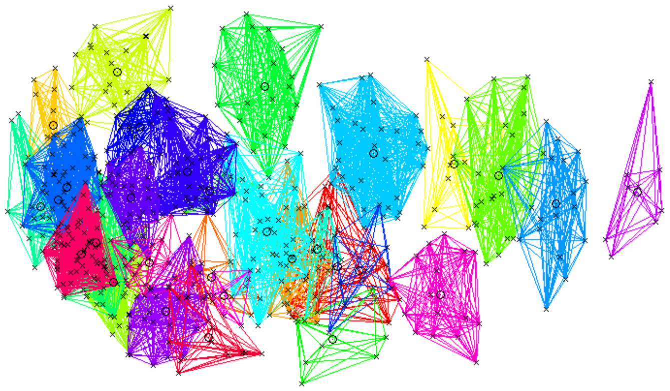

Figure 4 – Thirty-Clustering of P Data

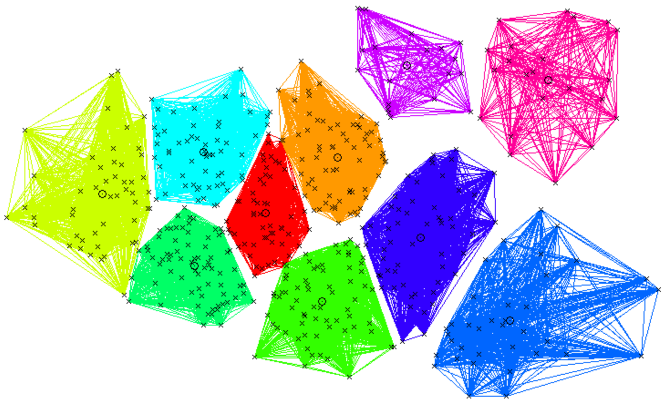

Figure 5 – Ten-Clustering of D Data

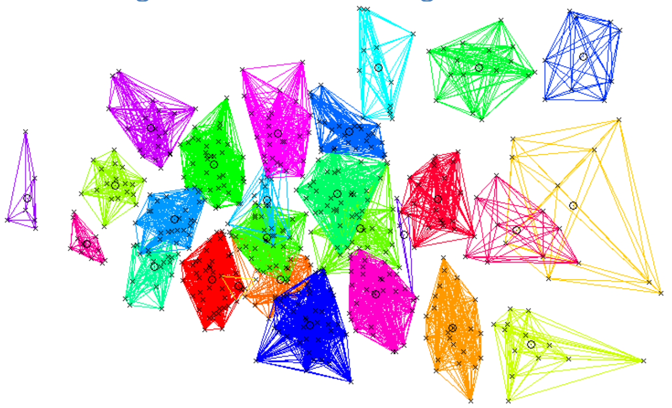

Figure 6 – Thirty-Clustering of D Data

VI. Qualitative Analysis of Partitions

A. Introduction

What sort of metric can be used to quantitatively say that a clustering of films is meaningful? One can only do this when using some measure of "closeness" between films. Having defined two such measures (ρ'_{mn} and d'_{mn}) in the decomposition step (see III) and used these values as inputs to our clustering algorithm, it would be tautological to say that the clusters we have created are successful partitions with respect to these metrics. Supposing the metrics used for decomposition are poor indicators of the film "closeness," our analysis would not observe poor clusterings of the data.

As such, we must look to a qualitative analysis of the film partitions. To do this, data from the Internet Movie Database (IMDB) were collected for each of the films in the product space. The average rating, budget, opening weekend gross, MPAA rating (i.e., R, PG-13, etc.), genres, directors, writers, and cast were then aggregated for each cluster as a means for qualitative comparison of the partitions.

B. Example Clusters

First, we will look at a cluster that provides a sanity check and reveals that the SOM methodology above generates at least some meaningful partitions. Example Cluster 1 (text box, next page) contains only eleven films, which is significantly fewer than 50, the average cluster size with ten partitions on 500 films. The extremely small size of the partition as compared to the average cluster size means that these eleven films must be very closely related and highly distinct from the other films in the product space.

Indeed, we see that six of these films are from the *Lord of the Rings* franchise (three Extended Edition DVD releases and three theatrical versions). The other films are also epic films, which are similar in scope and extravagance (not to mention, in length).

The average budget for these eleven films is on the high end of all clusterings at 73 million USD. The budgets of this cluster also have a low variance of 41 million dollars (relative to the budget size and compared to the other clusterings' budget variance) which can be accounted for by the change in value of the dollar since the *Star Wars* films came out.

These films were made to be giant blockbusters. All had extremely high opening weekend gross revenues, and these films have been seen by an extremely large portion of all moviegoers. Indeed, with the exception of *Sky Captain and the World of Tomorrow*, people also extremely enjoyed these movies (the *Lord of the Rings*

```
Cluster Size  :  11
              :
Titles        : LOTR: Fellowship                (4.435 +/- 0.895)
              : LOTR: Fellowship: Extended      (4.717 +/- 0.619)
              : LOTR: Return of King            (4.545 +/- 0.806)
              : LOTR: Return of King: Extended  (4.723 +/- 0.610)
              : LOTR: Two Towers                (4.461 +/- 0.862)
              : LOTR: Two Towers: Extended      (4.703 +/- 0.629)
              : Master and Commander            (3.546 +/- 0.986)
              : Raiders of the Lost Ark         (4.504 +/- 0.714)
              : Sky Captain and World of Tomor. (2.860 +/- 1.054)
              : Star Wars IV: A New Hope        (4.504 +/- 0.805)
              : Star Wars V: Empire Strikes Back(4.544 +/- 0.759)
              :
Rating Avg.   : 4.322
Stddev        : 0.807
              :
Budget        :  73.000  +/-   41.578 Mil. (11 reported)
Opening Gross :  36.071  +/-   28.924 Mil. (10 reported)
              :
MPAA Ratings  : PG-13 =  7
              :    PG =  3
              :
Genres        : 11 Action
              : 11 Adventure
              :  8 Fantasy
              :  3 Sci-Fi
              :  2 Thriller
              :  1 Drama
              :  1 Family
              :  1 Mystery
              :  1 War
              :
Director ( 6) : 0001392 Peter Jackson
              :
Writer   ( 6) : 0909638 Fran Walsh
              : 0866058 J.R.R. Tolkien
         ( 3) : 0000184 George Lucas
              :
Cast     ( 6) : 0089217 Orlando Bloom
              : 0101710 Billy Boyd
              : 0000949 Cate Blanchett
              : 0000276 Sean Astin
         ( 4) : 1019674 Sala Baker
              : 0032370 Noel Appleby
              : 0045324 John Bach
              : 0000293 Sean Bean
              : 0190744 Marton Csokas
              : 0384060 Bernard Hill
              : 0000489 Christopher Lee
         ( 3) : 0000148 Harrison Ford
```

Example Cluster 1
An example of an output cluster, from clustering P by a 10 neuron SOM

films top the list of the highest rated films). Indeed, this the films in this cluster have the largest aggregate average rating at 4.322 stars. Also worth noting is that people generally agree on the ratings of these films; the average standard deviation of the ratings of these eleven films is only 0.807 stars.

Lastly, there is an extremely high overlap of writers, directors, and cast members in these films, due to the fact that all six *Lord of the Rings* films were made by and with the same people.

Looking to Example Cluster 2, we see a markedly different type of movie represented by these films. Here we have, with very few exceptions, a cluster of thirteen romantic comedies (indeed, thirteen are listed under the ‘comedy’ genre by IMDB and 9 are under ‘romance’). These films have a relatively high budget and a decent opening weekend gross, but they are not as well liked as the successful epic blockbusters of Example Cluster 1. With an aggregate average rating of 3.381, this are the third least liked group of films in this partitioning. Furthermore, high variance in the ratings of these films may be explained by these movies “chick flick” status.

```
Cluster Size  :  13
              :
Titles        : Cheaper by the Dozen            (3.512 +/- 1.016)
              : Coyote Ugly                     (3.230 +/- 1.226)
              : How to Lose a Guy in 10 Days    (3.552 +/- 1.086)
              : Maid in Manhattan               (3.145 +/- 1.123)
              : Miss Congeniality               (3.361 +/- 1.112)
              : Miss Congeniality 2             (3.225 +/- 1.055)
              : Raising Helen                   (3.551 +/- 1.010)
              : Runaway Bride                   (3.291 +/- 1.056)
              : Sweet Home Alabama              (3.539 +/- 1.077)
              : The Princess Diaries            (3.571 +/- 1.046)
              : The Wedding Planner             (3.184 +/- 1.123)
              : Two Weeks Notice                (3.363 +/- 1.007)
              : What Women Want                 (3.425 +/- 1.069)
              :
Rating Avg.   : 3.381
Stddev        : 1.079
              :
Budget        :  49.167  +/-   11.654 Mil. (12)
Opening Gross :  21.886  +/-    8.227 Mil. (13)
              :
MPAA Ratings  : PG-13 = 10
              :    PG =  2
              :
Genres        : 13 Comedy
              :  9 Romance
              :  3 Drama
              :  2 Family
              :
Director ( 3) : 0005190 Garry Marshall
         ( 2) : 0677953 Donald Petrie
              :
Writer   ( 3) : 0492909 Marc Lawrence
         ( 2) : 0920859 Gina Wendkos
              : 0974301 Katie Ford
              :
Cast     ( 3) : 0000113 Sandra Bullock
              : 0122688 Heather Burns
```

Example Cluster 2
An example of an output cluster, from clustering P by a 30 neuron SOM

```
Cluster Size  :  20
              :
Titles        : 21 Grams                        (3.382 +/- 1.049)
              : 28 Days Later                   (3.335 +/- 1.118)
              : About Schmidt                   (3.059 +/- 1.071)
              : Amelie                          (4.115 +/- 1.033)
              : Bowling for Columbine           (3.785 +/- 1.202)
              : Closer                          (2.989 +/- 1.139)
              : Crouching Tiger, Hidden Dragon  (3.898 +/- 1.065)
              : Donnie Darko                    (3.925 +/- 1.064)
              : Fahrenheit 9/11                 (3.593 +/- 1.324)
              : Garden State                    (3.693 +/- 1.111)
              : High Fidelity                   (3.710 +/- 1.006)
              : In the Bedroom                  (3.290 +/- 1.066)
              : Napoleon Dynamite               (3.398 +/- 1.302)
              : Run Lola Run                    (3.887 +/- 1.004)
              : Secretary                       (3.423 +/- 1.153)
              : Super Size Me                   (3.864 +/- 0.974)
              : The Good Girl                   (3.109 +/- 1.022)
              : The Hours                       (3.351 +/- 1.141)
              : Traffic                         (3.693 +/- 0.988)
              : Whale Rider                     (3.915 +/- 1.017)
              :
Rating Avg.   : 3.571
Stddev        : 1.097
              :
Budget        :  11.463  +/-   13.093 Mil. (19)
Opening Gross :   2.588  +/-    5.663 Mil. (20)
              :
MPAA Ratings  : PG-13 =  3
              :     R = 15
              :    PG =  2
              :
Genres        : 16 Drama
              :  7 Comedy
              :  6 Romance
              :  5 Thriller
              :  3 Crime
              :  3 Documentary
              :  2 Action
              :  2 Sci-Fi
              :
Director ( 2) : 0601619 Michael Moore
              :
Writer   ( 2) : 0601619 Michael Moore
```

Example Cluster 3
An example of an output cluster, from clustering P by a 30 neuron SOM

Example Cluster 3 poses a more difficult analysis. With respect to movie topics and subject matter, there is little that relates these films to each other. These films include documentaries and journeys in science fiction. Some are disheartening postmodern character studies, while others are uplifting romantic comedies. Given the knowledge of the difference in these films' themes, has the partitioning scheme made an error?

Looking at this cluster from a different perspective reveals that there are ways to understand these movies with respect to each other. The average opening gross ranks in as the fourth lowest among all clusters. This indicates that these films were not initially well attended in theaters. This is generally true of these films—they are primarily movies with an indie following.

These are movies that have been very successful with one demographic group but no others. Michael Moore's films, *Bowling for Columbine* and *Fahrenheit 9/11*, are generally watched by many who are politically liberal and by few conservatives. Similarly, *Garden State* and *High Fidelity*, which express the youth generation's complaints about love and society, are generally watched by the 18-25 year old demographic.

There are four foreign films in this cluster (*Amelie*, *Crouching Tiger, Hidden* Dragon, *Run Lola Run* and *Whale Rider*), as well as three documentaries (*Bowling for Columbine*, *Fahrenheit 9/11* and *Super Size Me*). This cluster has an alternative feel, with films that are not out to please any large audience.

VII. Conclusion

The intangible quality of "indie-ness" that relates the films in Example Cluster 3 demonstrates power in the SOM algorithm. By many standards, these films would not be grouped similarly, and yet this group shares many features that could be very meaningful in analyzing the films for a collaborative filtering system.

It is important to note, however, that SOM clustering technique is also very successful with films that are easier to classify. Films with clearly defined features are separated along these lines (e.g., epics and romantic comedies are divided into Example Clusters 1 and 2, respectively). Additionally, films in the same franchise made in similar ways with similar casts are extremely rarely split into different clusters.

Further quantitative validity of these clusterings could be garnered via the empirical results of a collaborative filtering scheme that utilizes these partitions, such as the content-boosted system proposed by Melville, Mooney and Nagaraan [4]. Qualitatively, however, these clusters are consistent with the author's personal perspectives on these films, and seem to be very meaningful with respect to the content data gathered from IMDB on these films.

It seems that the problems of scalability can be mitigated by using this algorithm. The data considered in the calculations that arrive at these clusterings are much fewer than the entire set of viewer-movie rating pairs. Indeed, one only needs a single relational number between any two films in order to create meaningful partitions of some product space. Only one step of pre-processing must be done before clustering the films via the SOM algorithm.

In addition to being extremely useful for collaborative filtering algorithms [4, 5, 6], this work can be altered to be applicable in many fields. The problem of clustering is important for all sorts of computational algorithms and models (from pattern classification and data mining to resource allocation and strategic management). In order to extend this algorithm to other problems, the only thing necessary is some feedback on the items that one wants to partition and a measure of how the similar the items are as a function of all of their feedback.

Appendix A

Table 3 – Most Frequently Rated Films

Count	Rating	Title
233	3.361	Miss Congeniality
217	3.724	Independence Day
201	3.784	The Patriot
196	3.442	The Day After Tomorrow
194	4.154	Pirates of the Caribbean: Curse of the Black Pearl
193	3.905	Pretty Woman
182	4.300	Forrest Gump
181	4.307	The Green Mile
178	3.454	Con Air
178	3.412	Twister

Table 4 - Highest Rated Films

Rating	StdDev	Title
4.723	0.372	LOTR: Return of King, Extended
4.717	0.383	LOTR: Fellowship of Ring, Extended
4.703	0.396	LOTR: The Two Towers, Extended
4.593	0.459	Shawshank Redemption, Special Ed.
4.545	0.649	LOTR: Return of the King
4.544	0.577	Star Wars, V: Empire Strikes Back
4.504	0.622	The Godfather
4.504	0.648	Star Wars, IV: A New Hope
4.504	0.509	Raiders of the Lost Ark
4.461	0.638	Star Wars, VI: Return of the Jedi

Table 5 - Lowest Rated Films

Rating	StdDev	Title
2.798	1.003	The Stepford Wives
2.855	1.018	Hollow Man
2.856	1.196	Wild Wild West
2.860	1.110	Sky Captain and World of Tomorrow
2.901	1.639	Punch-Drunk Love
2.907	1.209	Legally Blonde 2
2.925	1.478	Anchorman
2.947	1.106	Once Upon a Time in Mexico
2.965	1.201	A.I. Artificial Intelligence
2.980	1.119	Daredevil

Table 6 – Films with Highest Rating Variance

Rating	StdDev	Title
3.593	1.752	Fahrenheit 9/11
3.398	1.697	Napoleon Dynamite
3.374	1.658	Moulin Rouge
3.280	1.656	The Royal Tenenbaums
2.901	1.639	Punch-Drunk Love
3.372	1.627	Lost in Translation
3.748	1.609	The Passion of the Christ
3.077	1.595	The Life Aquatic with Steve Zissou
3.230	1.503	Coyote Ugly
3.598	1.494	Sin City

Table 7 – Films with Lowest Rating Variance

Rating	StdDev	Title
4.723	0.372	LOTR: Return of King, Extended
4.717	0.383	LOTR: Fellowship of Ring, Extended
4.703	0.396	LOTR: The Two Towers, Extended
4.593	0.459	The Shawshank Redemption Special Ed.
4.504	0.509	Raiders of the Lost Ark
4.544	0.577	Star Wars, V: Empire Strikes Back
4.416	0.603	Finding Nemo
4.458	0.611	Schindler's List
4.173	0.617	Stand by Me
4.504	0.622	The Godfather

Table 8 - Films with Highest Correlation (ρ'_{mn})

Corr	Rating	Title
0.873	4.717 4.703	LOTR: Fellowship of Ring: Extended LOTR: The Two Towers: Extended
0.850	4.723 4.703	LOTR: Return of King: Extended LOTR: The Two Towers: Extended
0.839	4.723 4.717	LOTR: Return of King: Extended LOTR: Fellowship of Ring: Extended
0.814	4.435 4.461	LOTR: The Fellowship of the Ring LOTR: The Two Towers
0.801	4.092 4.045	Harry Potter and the Sorcerer's Stone Harry Potter and the Chamber of Secrets
0.785	4.545 4.461	LOTR: The Return of the King LOTR: The Two Towers
0.764	3.814 3.877	Lethal Weapon 3 Lethal Weapon 2
0.761	4.545 4.435	LOTR: The Return of the King LOTR: The Fellowship of the Ring
0.757	3.874 3.759	Kill Bill: Vol. 2 Kill Bill: Vol. 1
0.754	3.604 3.550	Star Wars, I: The Phantom Menace Star Wars, II: Attack of the Clones

Table 9 - Films with Lowest Correlation (ρ'_{mn})

Corr	Rating	Title
-0.267	3.280 3.398	The Royal Tenenbaums Pearl Harbor
-0.258	2.901 3.398	Punch-Drunk Love Pearl Harbor
-0.253	3.372 3.398	Lost in Translation Pearl Harbor
-0.253	3.725 3.583	Annie Hall Armageddon
-0.249	3.352 3.398	Adaptation Pearl Harbor
-0.241	3.372 3.583	Lost in Translation Armageddon
-0.239	3.725 3.398	Annie Hall Pearl Harbor
-0.237	3.280 3.583	The Royal Tenenbaums Armageddon
-0.235	2.901 3.640	Punch-Drunk Love Double Jeopardy
-0.234	2.901 3.583	Punch-Drunk Love Armageddon

Table 10 - Films of Highest Distance (d'_{mn})

Distance	Rating	Title
1.000	4.094 3.361	Pulp Fiction Miss Congeniality
0.964	4.300 3.361	Forrest Gump Miss Congeniality
0.952	3.280 3.361	The Royal Tenenbaums Miss Congeniality
0.951	3.963 3.361	American Beauty Miss Congeniality
0.948	3.280 4.300	The Royal Tenenbaums Forrest Gump
0.944	4.593 3.361	The Shawshank Redemption: Special Ed. Miss Congeniality
0.937	4.461 3.361	Lord of the Rings: Two Towers Miss Congeniality
0.936	4.307 3.361	The Green Mile Miss Congeniality
0.935	4.435 3.361	Lord of the Rings: Fellowship of the Ring Miss Congeniality
0.933	3.372 4.094	Lost in Translation Forrest Gump

Table 11 - Films of Lowest Distance (d'_{mn})

Distance	Rating	Title
0.124	4.717 4.703	LOTR: Fellowship of the Ring: Extended LOTR: Two Towers: Extended
0.131	4.723 4.703	LOTR: Return of the King: Extended LOTR: Two Towers: Extended
0.134	4.723 4.717	LOTR: Return of the King: Extended LOTR: Fellowship of the Ring: Extended
0.170	4.723 4.545	LOTR: Return of the King: Extended LOTR: Return of the King
0.187	3.609 3.790	Shall We Dance? In the Line of Fire
0.188	4.717 4.545	LOTR: Fellowship of the Ring: Extended LOTR: Return of the King
0.188	4.703 4.545	LOTR: Two Towers: Extended LOTR: Return of the King
0.190	3.766 3.609	Rules of Engagement Shall We Dance?
0.190	4.241 4.071	Rear Window Coach Carter
0.191	4.703 4.461	LOTR: Two Towers: Extended LOTR: Two Towers

ACKNOWLEDGMENT

A. Pariser would like to thank the Yale University Computer Science department for providing a venue to study this data, as well as Frederick Shic for helping focus the project. Thanks are also due to Daniel Spielman, who provided the author insight into ways to analyze clusters.

REFERENCES

[1] S. Harnad, "Cognition is Categorization", in Cohen, Henri and Lefebvre, Claire, Eds. Handbook of Categorization, Elsevier, 2005.
[2] S. Haykin, *Neural Networks: A Comprehensive Foundation* (Upper Saddle River, NJ: Prentice-Hall, 1999).
[3] E. Kreyszig, *Advanced Engineering Mathematics*, 8th Ed. (Hoboken, NJ: John Wiley & Sons, Inc., 1999).
[4] P. Melville, R.J. Mooney and R. Nagarajan, "Content-Boosted Collaborative Filtering for Improved Recommendations" in *Proceedings of the Eighteenth National Conference on Artificial Intelligence* (AAAI, 2002), pp. 187-192, Edmonton, Canada, July 2002.
[5] M. O'Connor and J. Herlocker, "Clustering Items for Collaborative Filtering" in *Proceedings of the ACM SIGIR Workshop on Recommender Systems*, Berkeley, CA, 1999.
[6] G.R. Xue, C. Lin, Q. Yang, et. Al., "Scalable Collaborative Filtering Using Cluster-based Smoothing" in *Proceedings of the 2005 ACM SIGIR Conference, Salvador, Brazil, 2005*, pp. 114-121

Face Recognition
A Comparative Study

Yan Sui

Computer Science Department, Yale University

***Abstract*—The conventional face recognition system consists of two parts: training and classification. The training part normally includes principle component analysis to reduce the dimensionality of images. In classification, a query image is projected to the reduced dimension and then compared with training images. Both training and classification could be done using neural networks' techniques. Specifically, PCA in the training phase could be done by neural network with Hebbian learning and the classification could also be done using a feed forward net. This paper compares the conventional techniques of face recognition with the techniques from neural networks.**

***Index Terms*—face recognition, eigenvalue, eigenvector, eigenface, principle component analysis, singular value decomposition, neural network, hebbian learning, feed forward net, backpropogation**

I. INTRODUCTION

FACE recognition has become a central technology for identity verification. Commercial systems are already widely used in access control and proactive surveillance applications all over the world.

Face recognition is not an easy task because of two major obstacles. Lighting conditions could significantly distort the content of the image. Makeup, hairdo and outfit could significantly change an individual's appearance. A pair of images of the same individual may look dramatically different. Such difficulties can make recognition extremely challenging. Moreover, difference in facial expressions also complicates the recognition problem. We shall, for simplicity, assume the lighting conditions are fairly constant. A good and robust face recognition system should work on faces with slight facial expressions. For convenience and simplicity, we only consider vertically oriented grey scale images.

Face recognition begins with a collection of labeled images. The label identifies the individual in the image. These labeled images, also called training images, are the bases for developing the recognition system. Typically, images are of size 100 pixels by 100 pixels, or more. For grey scale images, each pixel could take on any value between 0 and 255. Therefore, ten thousand dimensions of data need to be considered. Such high dimensionality of image data contributes to complexity of the problem. Since a large number of pixels could change their values due to a slight change in lighting and facial expression, recognition by comparing corresponding pixels in a pair of images is very inefficient and non-robust.

A more advanced face recognition system consists of two phases: training and classification. The first phase consists of training a system on a set of labeled images. The primary task of training is to reduce the dimensionality of the training images. Training is an offline process and it allows the classification phase, an online process, to perform comparisons among images in the reduced dimension.

To achieve the reduction of dimensions, the standard face recognition system uses principle component analysis (PCA). As well known, PCA presents the data in a way that maximizes the variance within the data. A nearest neighbor classifier could then be used to compare a pair of images in the reduced dimension by computing the Euclidean distance between them. The winner of this classification protocol is the labeled image that has the shortest distance from the target image in the reduced dimension.

Both the training and classification phases of the algorithm could be performed using neural networks. A neural network using Hebbian learning also produces the principle components. A feed forward net could be used in place of the nearest neighbor classifier in the classification phase.

Section II will present two different techniques for the training phase, namely the eigenface technique and the Hebbian learning neural network. Both are used to find the principle components. The classification could use either a nearest neighbor classifier or a feed forward net. These will be introduced in Section III. Since we have two options for training and two options for classification, there are total of four ways to construct the face recognition algorithm. In section IV, the performance of each of the four algorithms are presented and compared. The advantages and disadvantages of each option are discussed. Conclusion will be in section V.

II. Training

A. Eigenface

Principle component analysis, originated as a statistical analysis technique, identifies a way to represent high dimensional data in lower dimensions. The representation of the training images in lower dimensions is called the eigenfaces. See figure 3b). Eigenfaces have two important properties. The dimensions, or eigenfaces, are orthogonal to one another. A good estimate of the original data can be reconstructed by simply sum up the eigenfaces.

An outline of an algorithm to find eigenfaces from images is listed below:

1. For each training image i = 1 … m, place its pixels into a column vector x_i. m is the number of images.

2. Compute the mean face of the training images: µ
$$\mu = \frac{1}{m}\sum_{i=1}^{m} x_i$$
Figure 1 shows an example of the mean face.
3. Compute the covariance matrix: ∑
$$\Sigma = \frac{1}{m-1}\sum_{i=1}^{m}(x_i-\mu)(x_i-\mu)^T$$
4. Compute the eigenvalues and eigenvectors of the covariance matrix ∑
5. Choose the first K eigenvectors of ∑ that correspond to the largest K eigenvalues
6. Project the training images onto the principle component subspace of dimension K

Note in step 3, the covariance matrix has high dimensions, p by p, where p is the number of pixels in each image. It is memory intensive to compute such covariance matrix. Fortunately, eigenvectors can be computed without first computing the covariance matrix ∑, by using singular value decomposition (SVD).

If we combine the m column vectors into a matrix A
$$A = \begin{bmatrix} x_1 & x_2 & \dots & x_m \end{bmatrix}$$
and subtract the mean face µ from each training image
$$A = A - \mu$$
therefore, $\Sigma = AA^T$ (ignore the scalar $\frac{1}{m-1}$)

According to SVD, any m by n matrix A may be factored as the following:
$$A = USV^T$$
where U is of size m by m, S is of size m by n, and V is of size n by n. Also, the columns of U are the eigenvectors of AA^T. They are conveniently sorted by their corresponding eigenvalues, in descending order. The columns of V are the eigenvectors of A^TA. The diagonal of S are the singular values, or the square roots of the eigenvalues of AA^T, in descending order.

Therefore, the first K columns of matrix U are the same as the eigenvectors of the covariance matrix ∑ that correspond to the K highest eigenvalues.

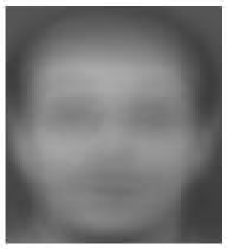

Figure 1. an example of mean face

B. Neural Network using Generalized Hebbian Algorithm

Besides eigenface, principle components can also be computed using neural network with Hebbian learning. A visualization of the neural network to compute the first K principle components is shown in figure 2.

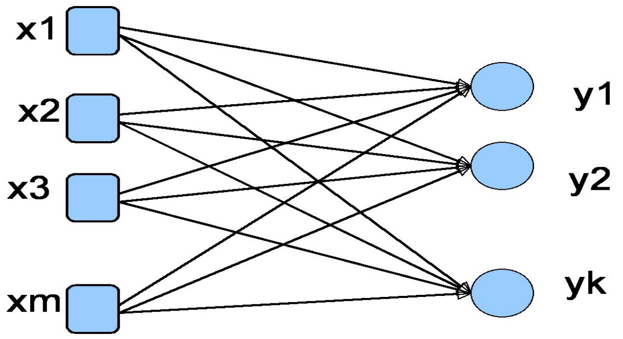

Fig 2. Neural Network for Hebbian Learning
Here m is number of pixels in each image

Here, there are m input nodes and k output nodes. m is the number of pixels in the images and k is the number of principle components to be computed. There is a weight value associated with each edge in the figure. The weights can be written in matrix form w. The following functions are used to update the weight matrix w.

$$y_j(n) = \sum_{i=1}^{m} w_{ji}(n) x_i(n) \qquad j = 1,2,...,k$$

$$\Delta w_{ji}(n) = \eta [y_j(n) x_i(n) - y_j(n) \sum_{p=1}^{j} w_{pi}(n) y_p(n)]$$

$$i = 1,2,...m \quad j = 1,2,...,k$$

Where η is the learning rate.

In the beginning, entries in the weight matrix w are initialized to small positive values. An iterative process to update the weight matrix w is used here. The training images are fed to the neural network, one at a time, repeatedly. After each iteration, the weights are updated. The process stops after the weights are stabilized. The weight matrix w is of size $m \times k$. The columns of w are the first k principle components. Or equivalently, the first column of weight matrix w is the first principle component. And the second column of w is the second principle component and so on.

For fast convergence, the following implementation issues need to be considered.

- Updating the learning rate. Gradually decrease the learning rate to ensure faster convergence.
- Testing for convergence. Every time after feeding all training images to the neural net, the change in weight matrix w is compared to a threshold value. Terminate the process if the change in the weight matrix is less than the threshold.

Both eigenface and Hebbian Learning produce principle components of the training images. But the number of dimensions to keep, or the value of K is a choice left for the user. In general, a larger K reserves more information from the original data and results in a smaller reconstruction error. At the same time, keeping more dimensions also produces more work to do in the classification phase. A good way to optimize the trade off between speed and accuracy is to look at the eigenvalues as in Figure 3 a). Here, K = 10 is a good choice due to the fact that eigenvalues drop off dramatically after the first 10. In essence, eigenvectors after the first 10 carry a lot less information than the first 10 eigenvectors and can be ignored. The visualization of the first 10 eigenfaces for a sample collection of faces is shown in Figure 3 b).

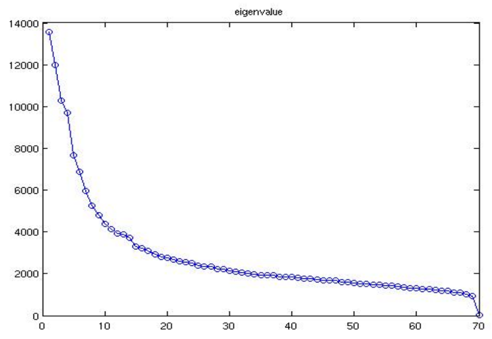

Fig. 3. a). Eigenvalues of a sample collection of images

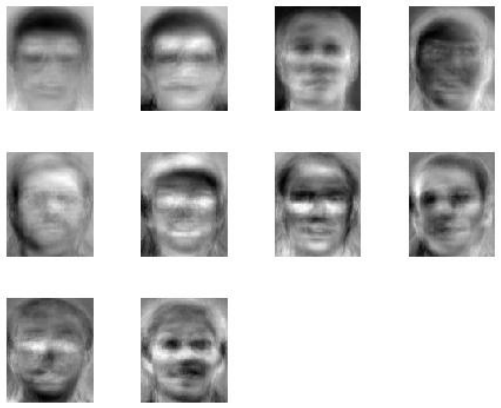

Fig. 3 b). First 10 eigenfaces or eigenvectors corresponding to the first 10 eigenvalues of a sample collection of images

As in

If the columns of matrix w are the principle components of the training images, each training image can be projected to lower dimensions by a simple multiplication.

$y_i = w \bullet x_i$

w is a matrix of size $k \times m$ and each row of w is a principle component. x_i is a vector of size $m \times 1$ containing the pixels of image i. y_i is the vector in the k dimensional space.

After all training images are projected to the subspace of dimension k, the next step is classification.

III. Classification

The goal of classification is to find the training image that best matches a query image. To find the best match, comparisons between the query image and each of the training images need to be performed. Note that all comparisons are done in the reduced dimension. A fast and easy way to do classification is to use nearest neighbor classifier.

A. Nearest Neighbor Classifier

The distance between an input image and a training image is computed as follows.

$$dist = \sqrt{\sum_{i=1}^{k} (train[i] - input[i])^2}$$

The difference in each dimension is squared and then added. The training image having the minimum distance from the query image is the best match.

This method is very simple and effective. Since the principle components are orthogonal to one another, the Euclidean distance between two points in the reduced dimension is a good measure of the difference between two images. As we will see in the next section, nearest neighbor classifier performs fairly well with PCA.

B. *Feed Forward Net*

The classifier could also be implemented using feed forward net. The idea is to train the feed forward net with the labeled training images. Use back-propagation to update the weights so that the neural net will recognize each training image. A visualization of the net is shown in Figure 4. Each training image is fed to the net only once. This process is a form of learning with a teacher, since the training images are all labeled.

In Figure 4, there are K input nodes in the input layer, representing the K principle components of the input data. In the output layer, there are C nodes, where C is the number of classes, or in this case, the number of different individuals in the training images. As in any feed forward net, the number of hidden layer is critical to performance. Having too few hidden layers results in inaccurate classification. On the other hand, too many hidden layers dramatically slow down the classification process. Some initial experiments show that two hidden layers is a good balance between speed and accuracy. The value at each output node represents the distance between the input and the node's corresponding class. If node yi has the minimum value, then class i is the best match to the input.

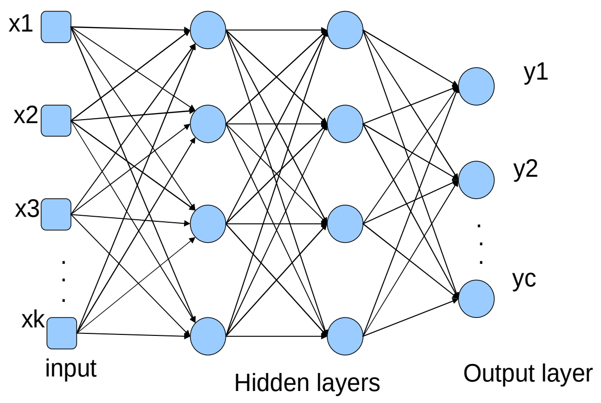

Fig. 4. Feed forward net with K input nodes, C output nodes, and two hidden layer each having K neurons

IV. Performance Evaluation

So far, two methods of computing PCA and two possible classifiers are introduced. There are a total of four possible combinations.

- Eigenface with nearest neighbor classifier
- Eigenface with feed forward net
- Hebbian learning with nearest neighbor classifier
- Hebbian learning with feed forward net

To illustrate to power and limitations of each of the four methods, experiments were conducted using the same data set for each of the four combinations. The images used were from AT&T laboratory at Cambridge University. In the database, there are images of 40 different people. Each individual has 10 images taken with slight lighting and facial expression changes. See Figure 5 for a snapshot of a subset of the database. The first seven images of each person were used as training images. All images were used as query images to test for accuracy.

Fig. 5. Images from database of AT&T laboratory at Cambridge University

The classification accuracy of the Hebbian learning with nearest neighbor and feed forward net are shown in Figure 6 and 7, respectively. K, the number of principle components used for classification, varies from 1 to 21 and the number of iteration to feed the training images to the neural net varies from 10 to 100. Note, the number of iteration is only an upper bound. The iterative process may end before it reaches this upper bound, if weights are stabilized early.

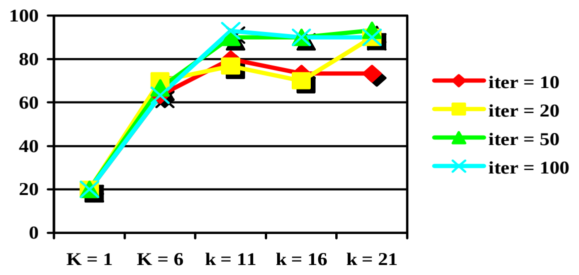

Fig. 6. Hebbian learning with nearest neighbor success rate as K and iteration vary

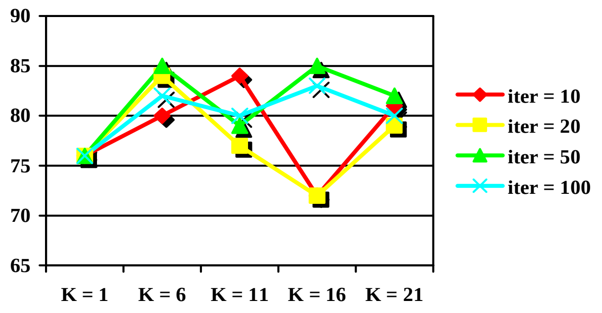

Fig. 7. Hebbian learning with feed forward net success rate as K and iteration vary. Note that in the case of feed forward net, the result is fairly consistent with different number of principle components.

For Hebbian learning with nearest neighbor classifier, accuracy gets better as the value of K and the number of iterations increases. The accuracy of Hebbian learning with feed forward net is relatively consistent as shown in figure 7. Notice that the accuracy in figure 7 is greater than 70% even when K = 1. This is due to feed forward net's ability to correctly recognize the training images.

The classification accuracy of eigenface with both nearest neighbor and feed forward net is given in figure 8.

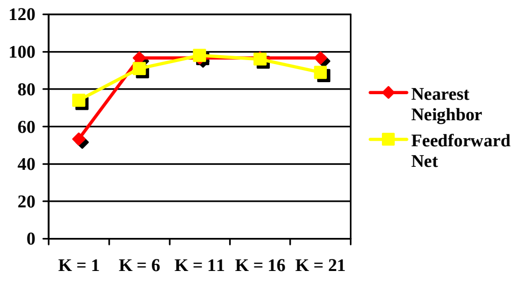

Fig. 8. Eigenface with nearest neighbor and feed forward net varying the value of K

We can plot the four combinations on the same graph to better visualize of the comparison, as shown in Figure 9.

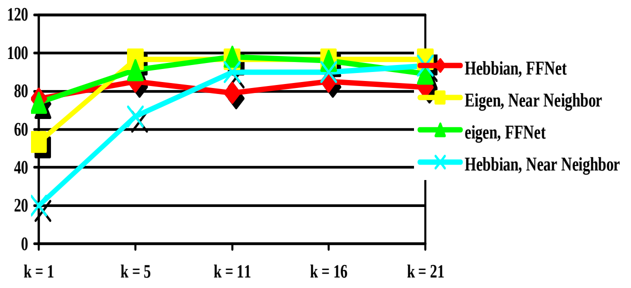

Fig. 9. Accuracy of all four combinations as K increases.
Note: Accuracy for Hebbian Learning is sampled at iteration = 50

Several interesting points to note:

- For the training phase, eigenface produces slightly higher accuracy. This is expected because hebbian learning is an iterative process that estimates the principle components. Errors in principle components need to be tolerated when using hebbian learning. Eigenface, on the other hand, finds the optimal solution in one shot.
- For classification, nearest neighbor does a slightly better job than feed forward net, when K >= 11. Feed forward net does a better job than nearest neighbor, when K < 11. This is due to the fact that nearest neighbor needs good results of PCA to work well. When K is large, more information about the data is captured in the principle components. Thus nearest neighbor performs better. Conversely, feed forward net does not require as much information to recognize the training images.

V. CONCLUSION

Face recognition, when assuming good lighting condition, is a well-researched problem. The simple and effective way to do face recognition is to use eigenface with nearest neighbor classifier. As shown in this paper, it works reasonably well. While face recognition can also be implemented using neural network techniques, it is not commonly used in this field. The major problem with neural network in face recognition is not the accuracy but speed. For both training and classification, neural network runs a lot slower than the simple eigenvector calculation. The iterative process of neural network limits its applicability to face recognition problems. In addition, as we discussed, when using neural network, there are a number of parameters that need to be carefully initialized and updated before and during the iterative process. This also makes the use of neural network more complicated and less desirable than eigenface.

Feed forward net recognizes the training images very accurately with little help from the training phase. It works exceptionally well in recognizing images it has seen before. For applications whose query images are a subset of its training images, feed forward net could be the leading candidate for classification.

Currently in face recognition, the query image needs to be compared to each and every training image in the training set during classification. If there are a large number of training images, the large number of comparisons will significantly reduce the speed of recognition system. Instead, the query image should only need to be compared with each class in the training set. For future studies in face recognition, instead of features describing each individual image, features describing each class or each individual person, should be investigated. This will greatly speed up the classification process.

In summary, face recognition could also be solved using techniques in neural networks. But the iterative process of neural networks needs a long time to converge. Nevertheless, there is potential in using neural network techniques in classification to improve the performance of face recognition.

ACKNOWLEDGMENT

I am grateful for the suggestions and help Professor Willard Miranker and teaching assistant Fred Shic have been giving me throughout the course of the project.

REFERENCES

[1] M. Turk and A. Pentland, "Face recognition using eigenfaces, " *Proc. IEEE Conf. on Computer Vision and Pattern Recognition*, 1991, pp. 586-591
[2] T. Kanade, *Computer Recognition of Human Faces*. Basel and Stuttgart: Birkhauser, 1977
[3] P. N. Belhumeur, J. P. Hespanha, and D. J. Kriegman, "Eigenfaces vs. fisherfaces: recognition using class specific linear projection," *IEEE Transactions on Pattern Analysis and Machine Intelligence*, vol. 19, no. 7, pp. 711-p20, July 1997
[4] A. L. Yuille, D. S. Cohen, and P. W. Hallinan, "Feature extraction from faces using deformable templates," *Proc. CVPR*, San Diego, CA June 1989

Note Onset Detection in Audio Sources

Andreas Voellmy (andreas.voellmy@yale.edu)

Abstract— **This paper presents the results of an investigation into note onset detection methods, in particular a note detection method using the high-frequency content of a signal and simple peak detection. The performance of this method is evaluated with sample audio in a variety of different musical styles. The advantages and disadvantages of this method are discussed and suggestions are made for further investigation into machine listening algorithms.**

Index Terms— **machine listening, note onset detection, beat tracking systems, audio.**

I. Introduction

NOTE onset detection, the temporal identification of note locations in audio sources, is an essential component in a variety of musical applications. Note detection is used in automatic transcription systems and real time musical applications, such as beat matching software for DJs and interactive performance of electronic music. Note onset detection is typically used in beat estimating applications, which use note onset events as inputs for the analysis of inter-note intervals and tempo estimation.

A variety of methods exist for detecting events in audio signals, some of which use neural nets [3]. This paper examines one such method, developed by Jensen and Anderson [2], that uses a single audio feature, the high frequency content. The simplicity of this method makes it suitable to real-time musical applications. The following sections describe the method and present the results of evaluating the method on a variety of musical examples.

II. Note Onset Detection Algorithm

Kristoffer Jensen and Tue Haste Anderson [2] developed a method for estimating the beat interval of musical audio which can be used in real-time musical applications to predict locations of beats. They have used this method in DJ software that automatically synchronizes two pieces of audio. In a first phase, the method uses a note onset detection algorithm to identify potential rhythmic markers in the audio source. In a second phase, the detected note onsets are used in a beat induction method that calculates the most probable beat intervals. This paper describes the note onset method.

The note onset detection method of Jensen and Anderson looks for peaks in the high frequency content of the audio source. High frequency content is a measure that emphasizes the higher frequencies, and is calculated by computing the discrete Fourier transform of an audio signal. It is defined as,

$$hfc = \sum_{n=0}^{B/2} a_n n^2 \tag{1}$$

where B is the block size of the audio segment, i.e. the number of samples in the audio segment, and a_n is the magnitude of frequency bin n. Jenson and Anderson define a time-varying high frequency content by computing the high frequency content over a window that slides over the audio signal. This can be defined as,

$$hfc(k_S) = \sum_{n=0}^{B/2} a_{n,k} n^2 \tag{2}$$

where k_S is an index into the audio signal stepping by S samples and $a_{n,k}$ is the magnitude of frequency bin n computed over B samples centered at $S \times k$, i.e. the samples from $S \times k - \frac{B}{2})$ to $S \times k + \frac{B}{2})$. Jensen and Anderson use a block size B of 2048 samples and step size S of 1024 samples, which they found to work optimally.

The time-varying high frequency content of the audio signal is then peak filtered to identify potential note onsets. The set of peaks is the set of block indexes, k, that satisfy the following criterion:

$$Peaks = \{k \mid hfc(k-1) < hfc(k) < hfc(k+1),\ hfc(k) > \theta\} \tag{3}$$

where θ is a threshold over which the peak must rise.

As an example, figure 1 shows an audio signal along with the high frequency content and peaks computed from it. Note that the audio signal and high frequency content are both normalized to the range $[-1, 1]$. The high frequency content clearly tracks this simple percussive signal closely.

While many peaks identified with this method correspond to appropriate rhythmic elements of the audio signal, others are spurious, i.e. they do not correspond to any perceivable note onsets. Such spurious peaks can be seen clearly in figure 2, which shows the analysis of a complex audio signal from a string quartet. The threshold θ helps to eliminate some of these spurious peaks. Unfortunately, raising the threshold to elimate spurious peaks often elimates real peaks.

Adding an event coalescing step significantly reduces the number of spurious peaks. The coalescing method merges peaks that occur within some time threshold δ of each other. The method replaces such pairs with the average of the pair and iterates over the peak set until a fixed point is reached. This can be described with more formally as,

$$Pairs(P) = \{(i, j) \mid |P_i - P_j| < \delta\} \tag{4}$$

$$Av(P) = \{\frac{i+j}{2} \mid (i, j) \in Pairs(P)\} \tag{5}$$

$$Spur(P) = \{i \mid (i, a) or (a, i) \in Pairs(P)\} \tag{6}$$

$$P_k = P_{k-1} \cup Av(P_{k-1}) - Spur(P_{k-1})\} \tag{7}$$

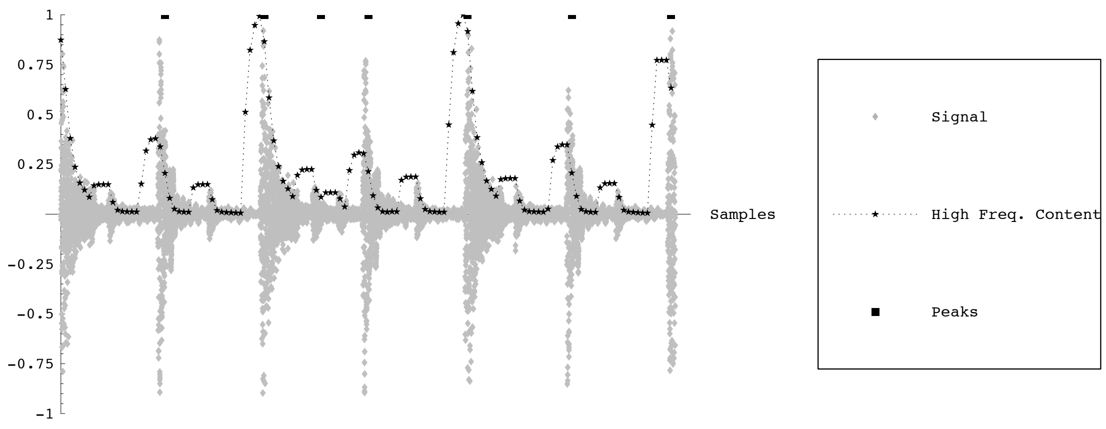

Fig. 1. Audio signal with high frequency content and peaks shown. Sample taken from Daft Punk song "Da Funk".

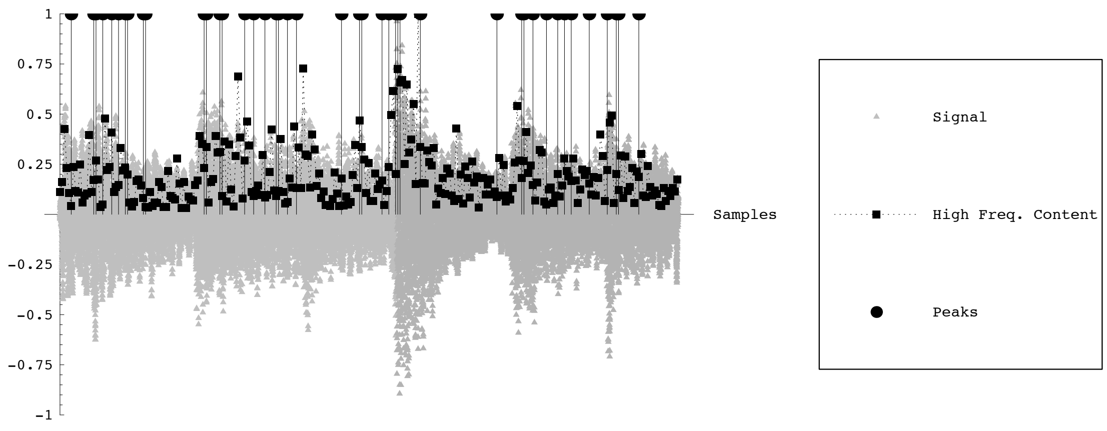

Fig. 2. Audio signal showing spurious peaks. Audio taken from a performance of Satie's Gymnopedies for solo piano.

III. Results

I evaluated the note detection method with a set audio signals from a variety of musical styles. The clips include simple clapping and percussion clips, solo piano, solo guitar and string quartet clips. In addition to the visual display (as seen in figures 1 and 2, I developed an auditory display in order to audition the quality of matching. This display creates a new audio clip with short reference tones inserted at every match point. This measure is very effective, because the human ear is very good at detecting accurate timing. By listening alone, it is clear that the note detection method is effective with simple and highly percussive music and much less effective with non-percussive music.

Furthermore, I developed a quantitative measure of success that compares detected note events with reference note events in audio clips. I manually analyzed a number of audio clips and determined the timing of each significant note event. These timings are not entirely precise and are assumed to have a tolerance of $\pm 15ms$.

The quality of note detections was judged on two criteria: the percent of reference notes found, and the ratio of the number of reference notes found to the total number of notes found. These measures are important because consumers of note event data will likely require a sufficient number of real detections without too many spurious detections confusing the signal. For example, Jensen and Anderson found that their beat estimation method required approximately 75% of events identified in order to perform adequately.

Because the performance generally depends on the value of the threshold θ used, we let P_θ be the set of detections at some threshold θ, P_{ref} be the set of reference events, and ϕ be the error resolution of the reference events and formalize these criteria as:

$$MatchingP_\theta = \{p \mid p \in P_\theta, \exists j \in P_{ref}. |j - p| < \phi\} \quad (8)$$

$$RefsFound_\theta = \frac{|MatchingP_\theta|}{|P_{ref}|} \quad (9)$$

$$NonSpurious_\theta = \frac{|RefsFound_\theta|}{|P_\theta|} \quad (10)$$

I also define a measure of the most peaks matched, that is, the number of peaks matched with zero threshold:

$$MaxMatched = |MatchingP_{\theta=0}| \tag{11}$$

These numeric measures can be used to confirm the result that this note detection method works better for percussive music than for non-percussive music, as can be seen in Table I.

I found that note detection is highly sensitive to threshold selection, though slightly less sensitive in simple, percussive music. This can be seen in figures 3 and 4, which show note detections as a function of threshold for clips of simple percussion and solo guitar respectively. The method performs more poorly on the solo guitar clip overall, and reaches 0 detections more quickly.

Figures 3 and 4 also show the effect of the coalescing step of the algorithm, by showing $NonSpurious_\theta$ for peaks with and without coalescing. In figure 3 coalescing typically eliminates all non-spurious detections, while in figure 4 coalescing only eliminates non-spurious detections at very low threshold levels.

IV. Discussion

The note onset detection method of Jensen and Anderson appears to perform better on simple percussive music and worse on complex or non-percussive music. It also tends to be very sensitive to the threshold parameter and generates many spurious detections.

However, the performance may still be adequate for many uses. For example, beat estimation methods may perform adequately with many missed notes and spurious detections. Jensen and Anderson's beat estimation procedure involves the construction of a probability vector of inter-onset intervals. This probability vector may still tend to indicate a reasonable tempo despite numerous missed events.

On the other hand, the performance is not sufficient for automated music transcription purposes or other uses requiring a high degree of accuracy and precision. Other methods, such as the neural net-based approach used in Marolt, Kavcic, and Privosnik [3], may perform better for such tasks.

Due to the limited number of reference audio clips used in this investigation, these preliminary results can only be interpreted as indications of performance. A much larger set of reference clips should be used in order to fully evaluate and quantify the performance of this, and other, note detection methods. Producing high quality event timings on audio clips is a time-consuming manual task. Further work should identify a database of such reference clips or work to create such a reference database. Such a database would be useful for the quantitative comparison of the many published note onset detection methods. Typically, no inter-method comparisons are published, making it difficult for choose a method for a particular use.

Further work should be done to compare the performance of using high-frequency content with using simple audio amplitude. Using amplitude is the simplest approach to note detection and would establish a reference point for other methods.

A more serious problem with the general approach of note onset detection lies in how to define a note onset or an event. Though the definition of events in extremely simple percussive music is fairly clear, such a definition is difficult to make for most music. Most music has overlapping and complex events, with multiple levels of detail. Human listeners may have difficulty identifying individual events and may require careful, repeated listening to perceive events. Different listeners may interpret events differently, with expert listeners identifying finer details of the music.

Despite these difficulties in detecting note onsets, humans have no trouble tracking beat and tempo and precisely coordinating their actions with musical audio. This suggests that detecting note onsets is not essential to both temporal coordination and beat perception, and it suggests that the mechanisms may be somewhat independent. It also suggests that detecting note onsets may be useful in only a small number of cases, and that other methods of processing audio are useful for most tasks. Indeed, a beat tracking system built by Eric Scheirer [4] estimates beats without identifying note onsets. The method processes audio directly, using resonant filters to identify probable rhythmic pulses. This method draws on psychoacoustic experiments that show that some audio signal simplificationspreserve listeners perception of pulse and rhythm. One example of such a transformation is “amplitude-modulated noise” in which white noise is resynthesized with the amplitude envelopes of an original signal in a few (4-6) frequency bands.

V. Conclusions

Note onset detection can be performed adequately for simple, percussive audio signals by applying a thresholded peak detection algorithm to the time-varying high frequency content of a signal. Note onsets are much more difficult to define in most musical audio sources. Fortunately, for most applications of machine listening, accurate note onset are probably not required. I am interested in investigating the neural mechanisms for the psychoacoustic properties of rhythm and pulse. Such understanding may lead to more effective algorithms for machine understanding of rhythm in audio sources.

References

[1] K. Jensen and T.H. Andersen. Beat estimation on the beat. In IEEE Workshop on Applications of Signal Processing to Audio and Acoustics, 2003.

[2] K. Jensen and T. H. Andersen, ”Real-time beat estimation using feature extraction,” in Proceedings of the Computer Music Modeling and Retrieval Symposium, ser. Lecture Notes in Computer Science. Springer Verlag, 2003.

[3] Matija Marolt, Alenka Kavcic, and Marko Privosnik. Neural networks for note onset detection in piano music. In Proc. Int. Computer Music Conference, Gothenberg, Sweden, 2002.

[4] E. D. Scheirer, ”Tempo and beat analysis of acoustic musical signals,” J. Acoust. Soc. Am., vol. 103, no. 1, pp. 588–601, January 1998.

TABLE I
EVENTS MATCHED BY REFERENCE CLIP

Clip	Description	MaxMatched
Clap3.aif	monophonic clap	1.0
DaFunk-Short-1.aif	simple percussive	1.0
DaFunkFill-Short-1.aif	simple percussive, high-pass filtered	0.67
Starobin-Short-1.aif	solo guitar	1.0
Satie-Gymno-Short-1.aif	solo piano, chords	0.5
Schiff-Goldberg-Short-1.aif	solo piano, two voice counterpoint	0.77
Kronos-Glass-Short-1.aif	string quartet	0.67

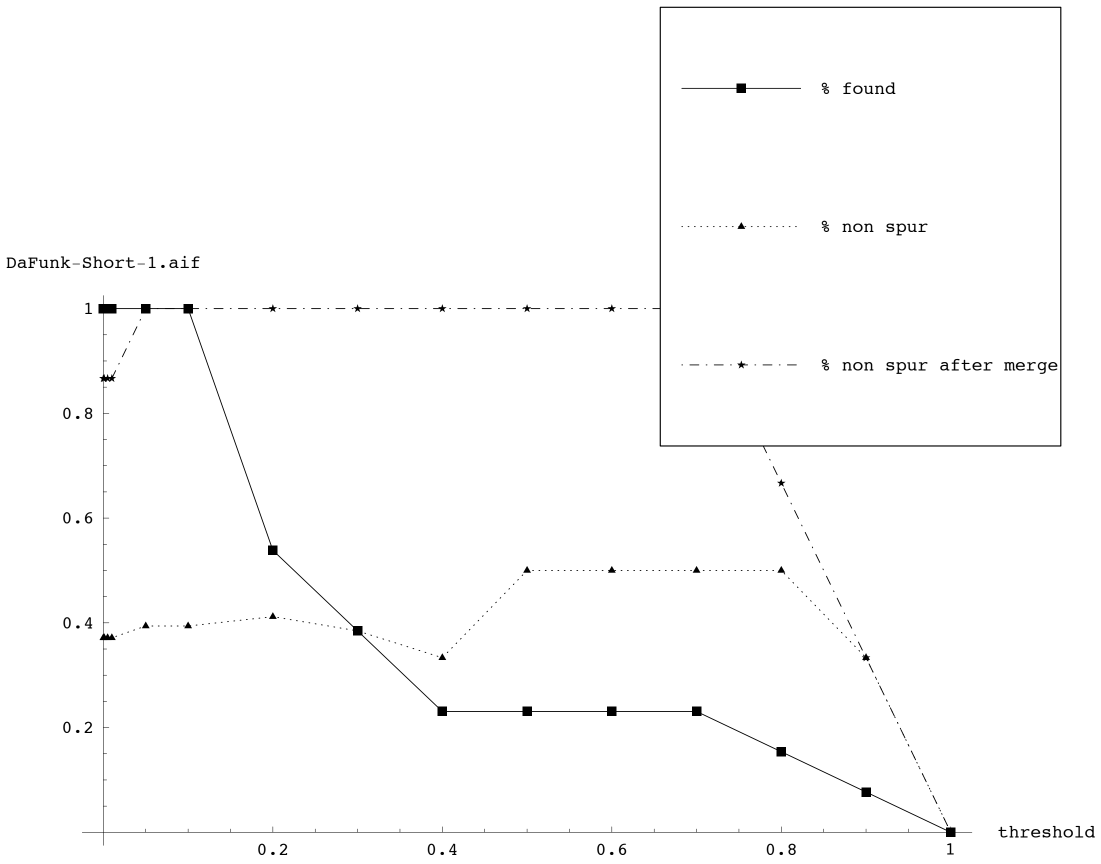

Fig. 3. Detection quality as a function of threshold for a simple percussive audio clip.

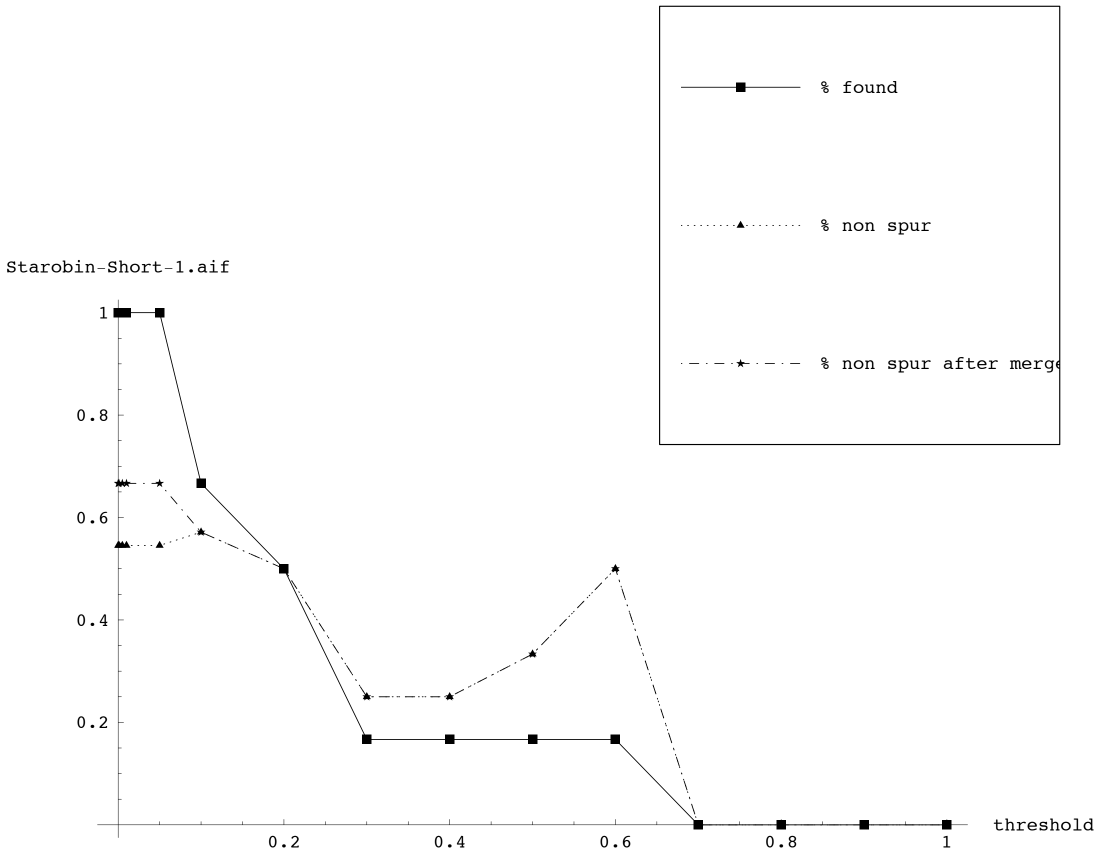

Fig. 4. Detection quality as a function of threshold for a solo guitar audio clip.